Supplementary Material for

Heterobimetallic complexes composed of bismuth and lithium carboxylates as polyurethane catalysts – alternatives to organotin compounds

Emre Levent[†], Oliver Sala[‡], Lukas F.B. Wilm[†], Pawel Löwe[†] and Fabian Dielmann[†#*]

† Institut für Anorganische und Analytische Chemie, Westfälische Wilhelms-Universität Münster
Corrensstrasse 30, 48149 Münster (Germany)

‡ BASF SE, Carl-Bosch-Straße 38, 67063 Ludwigshafen am Rhein

Institut für Allgemeine, Anorganische und Theoretische Chemie, Leopold-Franzens-Universität
Innsbruck, Innrain 80-82, 6020 Innsbruck (Austria)
email: fabian.dielmann@uibk.ac.at
Homepage: https://www.uibk.ac.at/aatc/mitarbeiter/dielmann/

CONTENTS:

Synthetic Details

General remarks: All manipulations were performed under an inert atmosphere of dry argon, using standard Schlenk and drybox techniques. Dry and oxygen-free solvents were employed. ^{1}H, and ^{13}C spectra were recorded at 300 K on Bruker AVANCE I 400, Bruker AVANCE III 400, AVANCE Neo 500SB or Bruker AVANCE II 200 spectrometers. DOSY measurements were recorded at 300 K on Agilent DD2 500. Low temperature NMR spectra were recorded on a Bruker AVANCE III 400 spectrometer at the temperatures indicated. All other spectra were obtained at 25 °C in the solvent indicated. Chemical shifts are given in parts per million (ppm) relative to SiMe$_4$ (^{1}H, ^{13}C) and were referenced internally to the residual solvent signals. NMR multiplicities are abbreviated as follows: s = singlet, d = doublet, t = triplet, q = quartet, p = quintet, sept = septet, m = multiplet, br = broad signal. Mass spectra were obtained with an Orbitrap LTQ XL (Thermo Scientific) spectrometer. IR spectra were obtained on a Bruker ALPHA II FT-IR spectrometer.

Triphenyl bismuth (BiPh$_3$) was prepared by following the literature procedure.[1] All other compounds were purchased from commercial sources. Pivalic acid and 2,2-dimethyl butyric acid were dried over P_4O_{10} and subsequently distilled, 2-phenylisobutyric acid was purified by sublimation.

Preparation of bismuth(III) carboxylates **1-3**

General procedure 1 (GP1): The bismuth(III) carboxylates were prepared following a modified synthetic procedure of Andrews *et al.*[2] A Schlenk flask was charged with BiPh$_3$ (1.00 eq.) and the carboxylic acid (3.00 eq.). Anhydrous toluene (3 mL per mmol of BiPh$_3$) was added and the reaction mixture was heated for at least 16 hours at 110 °C. The complete consumption of BiPh$_3$ was determined by ^{1}H NMR monitoring of the reaction mixture. Subsequently, all volatiles where removed under reduced pressure and the residue was dried *in vacuo* at 80 °C overnight to afford the bismuth(III) carboxylate as an off-white solid.

Compound 1: Synthesis according to **GP1** starting from BiPh$_3$ (3.92 g, 8.90 mmol) and pivalic acid (3.00 mL, 26.70 mmol). Yield 99 % (4.51 g, 8.81 mmol) as a white solid.
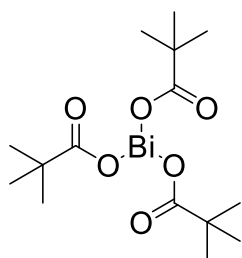
^{1}H NMR (400.13 MHz, CD$_2$Cl$_2$): δ = 1.20 (s, 27H, CH$_3$).

^{13}C{^{1}H} NMR (100.62 MHz, CD$_2$Cl$_2$): δ = 190.0 (s, COO), 42.8 (s, C(CH$_3$)$_3$), 27.3 (s, CH$_3$).

HRMS (ESI): m/z calculated for [C$_{15}$H$_{27}$BiO$_6$] (Na)$^+$ 535.1504, found 535.1502 [Bi(piv)$_3$+Na]$^+$.

Elemental analysis: calculated (%) for C$_{15}$H$_{27}$BiO$_6$: C 35.16, H 5.31, found C 34.75, H 5.25.

IR (neat): $\tilde{v}$ = 2965 (s), 2930 (m), 2905 (m), 2871 (m), 1580 (s), 1538 (s), 1479 (vs), 1459 (s), 1403 (vs), 1357 (vs), 1216 (s), 908 (w), 893 (w), 814 (w), 804 (w), 786 (w), 609 (m), 546 (w), 416 (w) cm^{-1}.
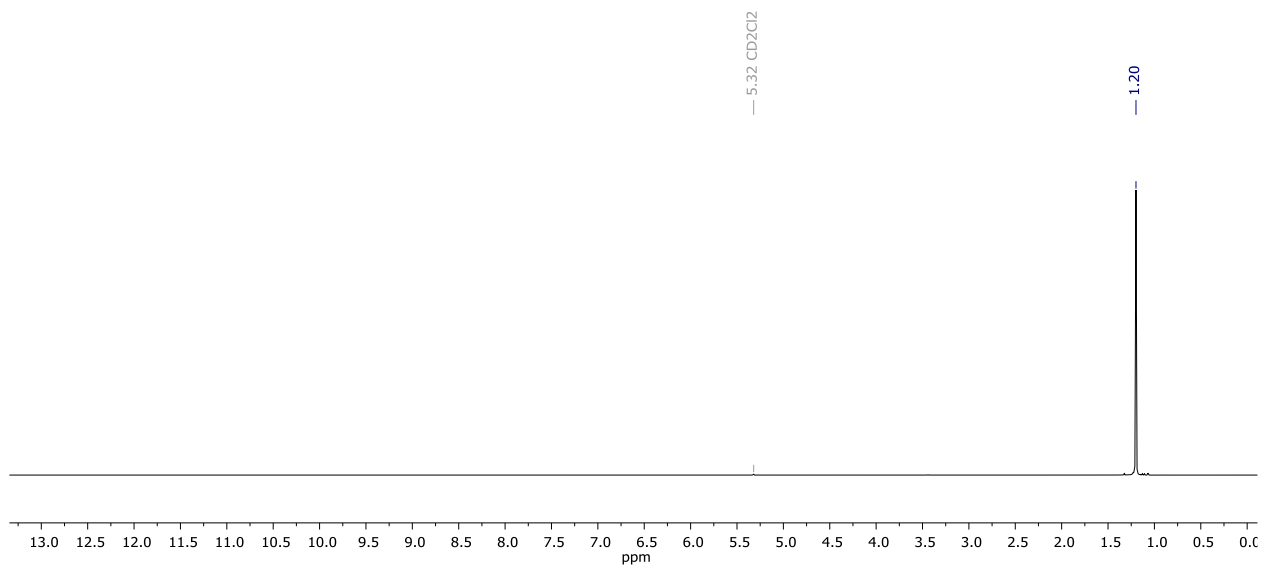
Figure S1: ^{1}H NMR spectrum (in CD$_2$Cl$_2$, 300 K, 500.23 MHz) of bismuth pivalate (**1**).
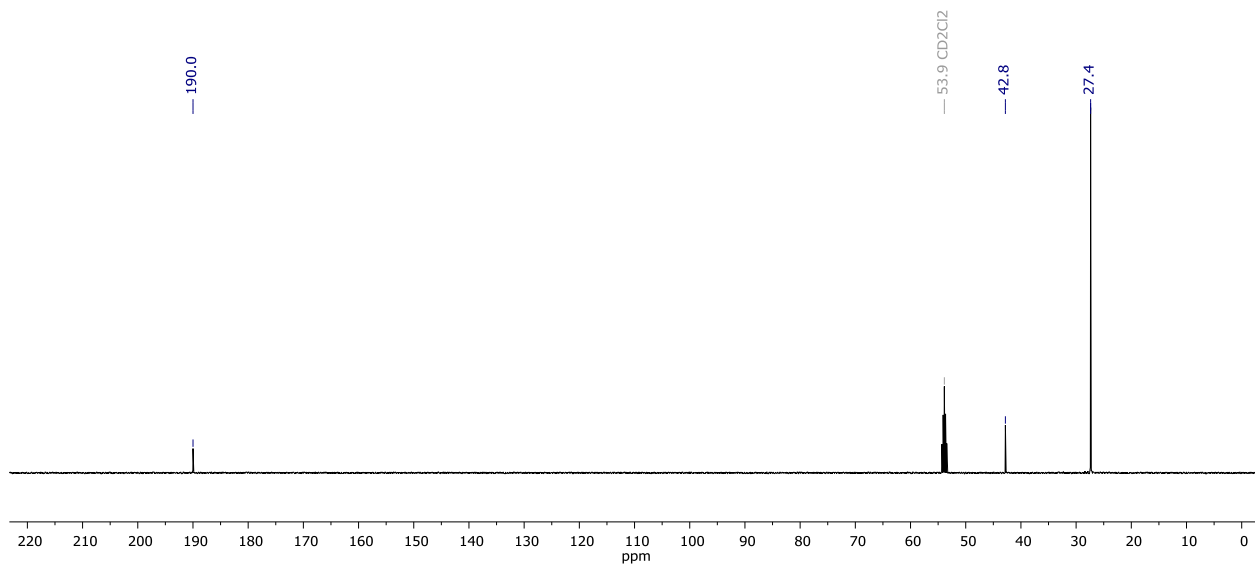
Figure S2: ^{13}C{^{1}H} NMR spectrum (in CD$_2$Cl$_2$, 300 K, 300 K, 125.80 MHz) of bismuth pivalate (**1**).

Compound 2: Synthesis according to **GP1** starting from BiPh$_3$ (3.50 g, 7.95 mmol) and 2,2-dimethylbutyric acid (3.00 mL, 23,85 mmol). Yield 99 % (4.36 g, 7.87 mmol) as a white solid.
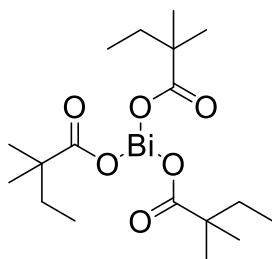
^{1}H NMR (400.13 MHz, CD$_2$Cl$_2$): δ = 1.57 (q, $^3J_{HH}$ = 7.5 Hz, 6H, CH$_2$(CH$_3$)), 1.14 (s, 18H, CH$_3$), 0.90 (t, $^3J_{HH}$ = 7.5 Hz, 9H, CH$_3$(CH$_2$)).

^{13}C{^{1}H} NMR (100.62 MHz, CD$_2$Cl$_2$): δ = 189.4 (s, COO), 46.7 (s, C(CH$_3$)$_2$), 34.0 (s, CH$_2$C), 24.9 (s, (CH$_3$)$_2$C), 9.7 (s, CH$_3$).

HRMS (ESI): m/z calculated for [C$_{18}$H$_{33}$BiO$_6$] (Na)$^+$ 577.1973, found 577.1967 [Bi(dmb)$_3$+Na]$^+$, 917.2276 (917.2276) [Bi$_2$(dmb)$_4$+K]$^+$.

Elemental analysis: calculated (%) for C$_{18}$H$_{33}$BiO$_6$: C 38.99, H 6.00, found C 38.56, H 6.08.

IR (neat): $\tilde{v}$ = 2968 (vs), 2930 (m), 2880 (m), 1702 (w), 1527 (vs), 1475 (s), 1461 (s), 1395 (vs), 1358 (vs), 1327 (w), 1284 (s), 1200 (m), 1182 (m), 1065 (w), 1008 (w), 935 (w), 891 (m), 810 (m), 793 (w), 767 (w), 642 (w), 599 (m), 534 (W), 499 (w), 459 (w) cm^{-1}.
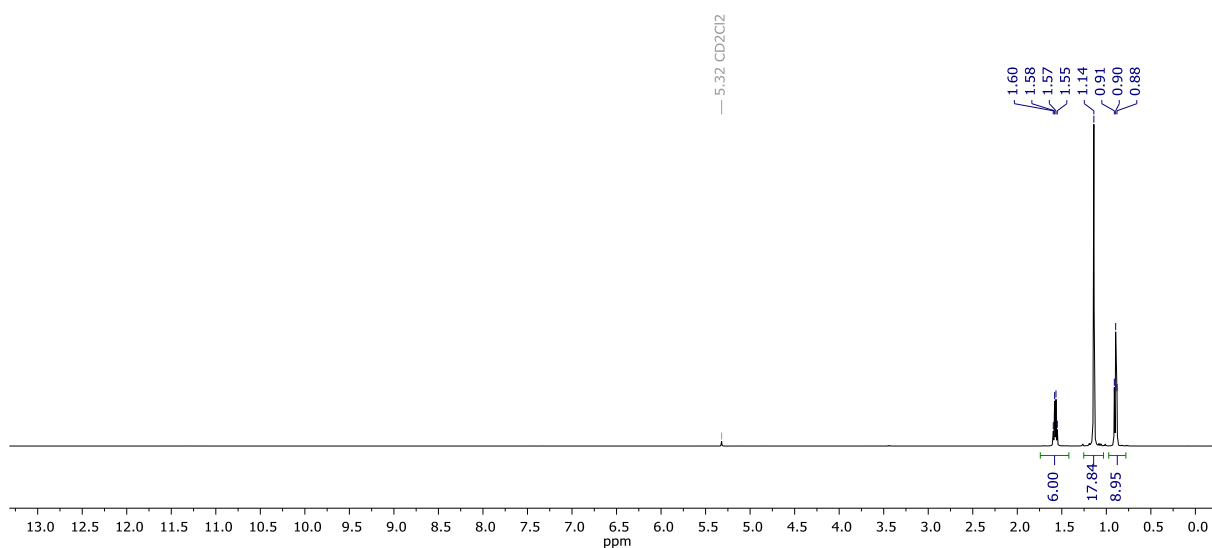
Figure S3: ^{1}H NMR spectrum (in CD$_2$Cl$_2$, 300 K, 400.13 MHz) of bismuth 2,2-dimethylbutyrate (**2**).
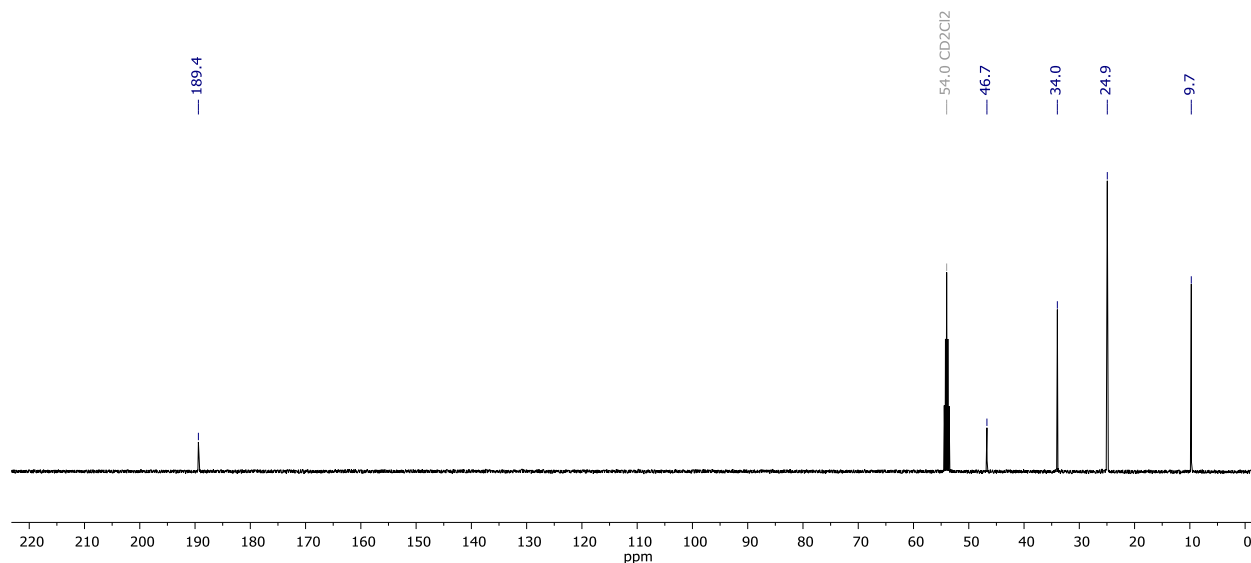
Figure S4: $^{13}C\{^1H\}$ NMR spectrum (in CD_2Cl_2, 300 K, 300 K, 100.62 MHz) of bismuth 2,2-dimethylbutyrate (**2**).

Compound 3: Synthesis according to **GP1** starting from $BiPh_3$ (3.50 g, 7.95 mmol) and 2-phenylisobutyric acid (3.92 g, 23,85 mmol). Yield 99 % (5.50 g, 7.87 mmol) as a white solid.
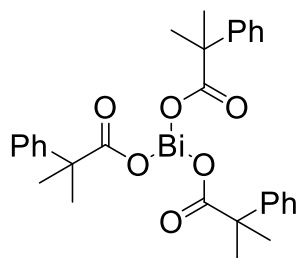
^{1}H NMR (400.13 MHz, CD_2Cl_2): δ = 7.37 (m, 6H, aryl-H), 7.29 (m, 6H, aryl-H),7.21 (m, 3H, aryl-H), 1.51 (s, 18H, CH_3)

$^{13}C\{^1H\}$ NMR (100.62 MHz, CD_2Cl_2): δ = 187.6 (s, COO), 145.3 (s, *ipso*-C), 129.0 (s, aryl-C), 127.4 (s, aryl-C), 126.8 (s, aryl-C), 50.9 (s, $C(CH_3)_2$), 26.6 (s, CH_3).

HRMS (ESI): m/z calculated for $[C_{20}H_{22}BiO_4]^+$ 535.1317, found 535.1335 $[Bi(pib)_2]^+$, 721.1999 (721.1973) $[Bi(pib)_3+Na]^+$, 907.2665 (907.1880) $[Bi_2(pib)_3]^+$, 1233.3451 (1233.3397) $[Bi_2(pib)_5]^+$, 1419.4111 (1419.4054) $[Bi_2(pib)_6+Na]^+$.

Elemental analysis: calculated (%) for $C_{30}H_{33}BiO_6$: C 51.58, H 4.76, found C 51.56, H 4.60.

IR (neat): $\tilde{\nu}$ = 3088 (w), 3058 (w), 3026 (w), 2968 (m), 2930 (m), 2873 (w), 1589 (w), 1521 (vs), 1498 (m), 1474 (m), 1443 (w), 1396 (vs), 1360 (vs), 1333 (m), 1207 (w), 1237 (w), 1182 (m), 1103 (w), 1077 (w), 1029 (w), 950 (w), 882 (m), 837 (w), 795 (w), 766 (w), 754 (w), 738 (m), 694 (m), 647 (m), 564 (w), 504 (w), 477 (w), 428 (w) cm^{-1}.
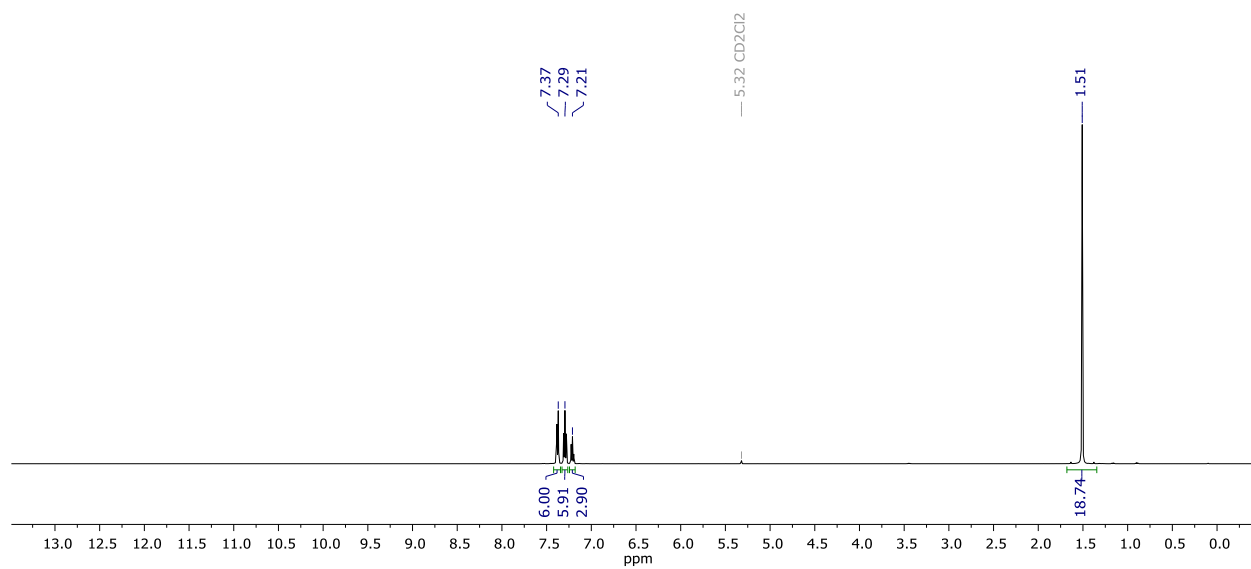
Figure S5: ^{1}H NMR spectrum (in CD_2Cl_2, 300 K, 400.13 MHz) of bismuth 2-phenylisobutyrate (**3**).
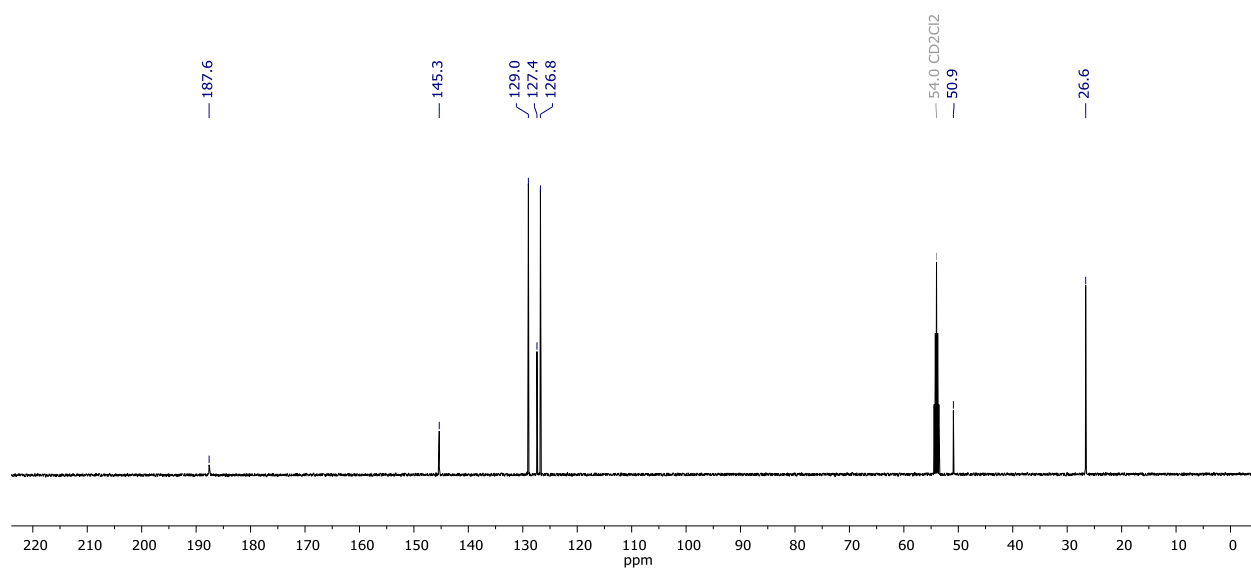
Figure S6: $^{13}C\{^1H\}$ NMR spectrum (in CD_2Cl_2, 300 K, 300 K, 100.62 MHz) of bismuth 2-phenylisobutyrate (**3**).

Preparation of lithium carboxylates 4-6

General procedure 2 (GP2): Preparation of lithium carboxylates. A Schlenk flask was charged with the carboxylic acid (1.00 eq.) and anhydrous *n*-hexane (80 mL). The reaction mixture was cooled to -80 °C and a 1.6 M solution of *n*-butyllithium in *n*-hexane (1.00 eq.) was added dropwise. The resulting suspension was warmed up to room temperature and stirred for 2 hours. Afterwards the suspension was filtered and washed 3 times with 25 mL diethyl ether. After drying at 100 °C *in vacuo* overnight, the lithium salt was obtained as a white solid in quantitative yield.

Compound 4: Synthesis according to **GP2** starting from pivalic acid (7.00 mL, 62.5 mmol) and *n*-butyllithium (39.00 mL, 62.5 mmol, 1.6°M). Yield: quantitative (6.70 g, 62.5 mmol), white solid.
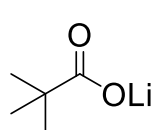
^{1}H NMR (400.13 MHz, dmso-d_6): δ = 1.00 (s, 9H, CH$_3$).

^{13}C\{^{1}H\} NMR (125.80 MHz, dmso-d_6): δ = 182.7 (s, COO), 38.4 (s, C(CH$_3$)$_3$), 28.7 (s, CH$_3$).

^{7}Li\{^{1}H\} NMR (155.47 MHz, dmso-d_6): δ = -0.10 (s, br).

Elemental analysis: calculated (%) for C$_5$H$_9$LiO$_2$: C 55.57, H 8.39, found C 54.99, H 8.50.

IR (neat): $\tilde{v}$ = 2984 (w), 2959 (m), 2930 (w), 2906 (w), 2871 (w), 1610 (m), 1569 (vs), 1525 (s), 1482 (s), 1417 (s), 1374 (m), 1360 (s), 1226 (m), 1029 (w), 938 (w), 894 (w), 597 (w), 557 (w) cm^{-1}.
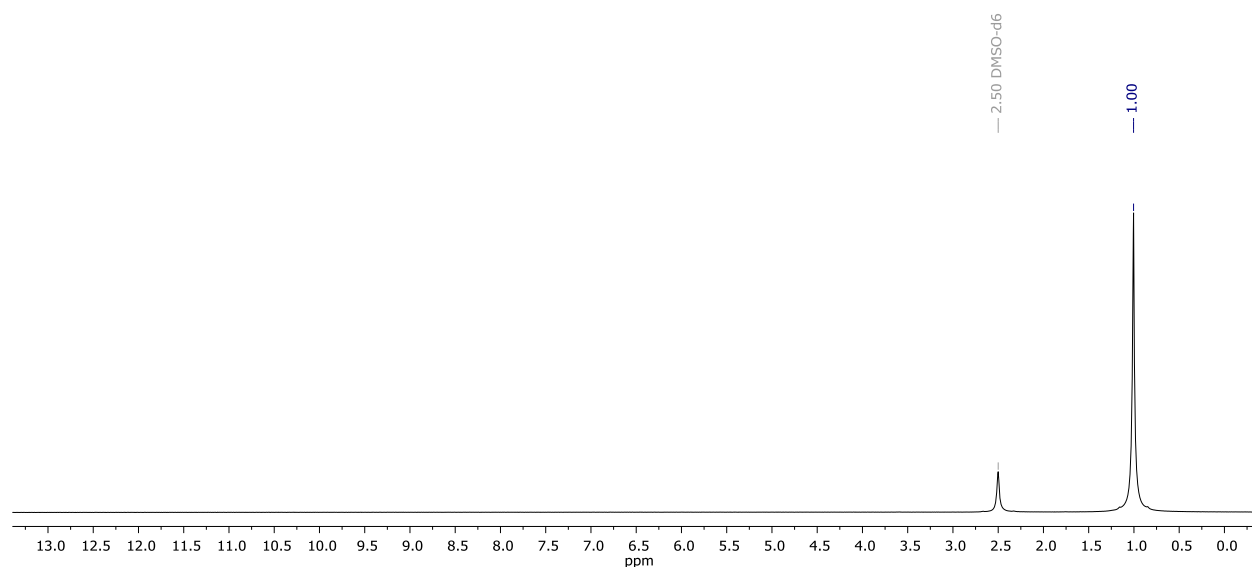
Figure S7: ^{1}H NMR spectrum (in dmso-d_6, 300 K, 400.13 MHz) of lithium pivalate (**4**).
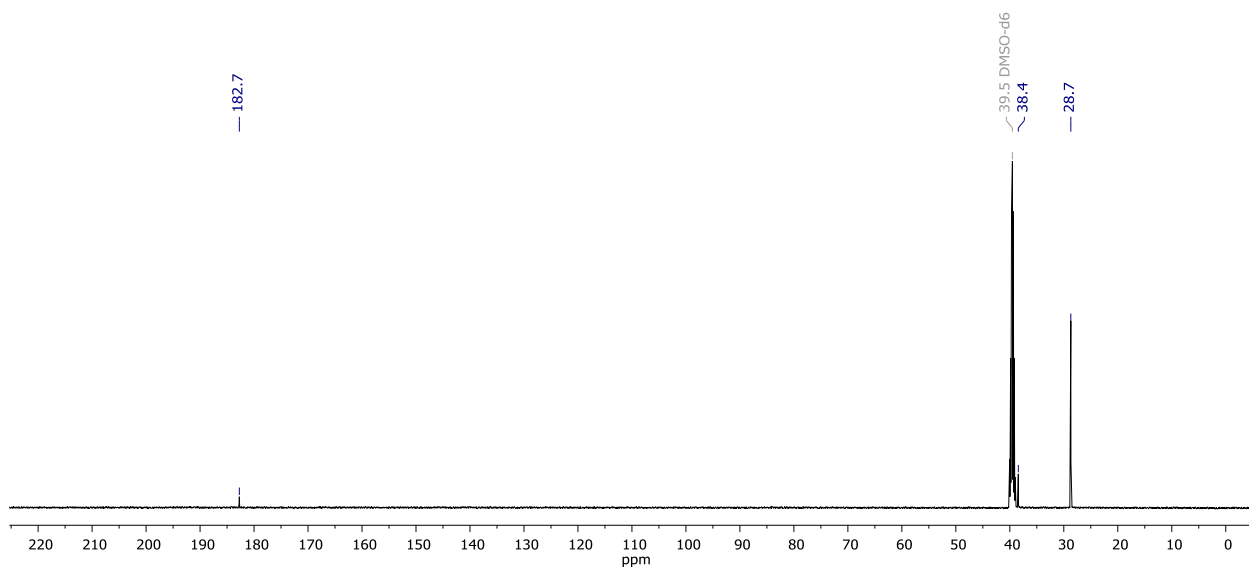
Figure S8: $^{13}C\{^{1}H\}$ NMR spectrum (in dmso-d$_6$, 300 K, 300 K, 125.80 MHz) of lithium pivalate (**4**).
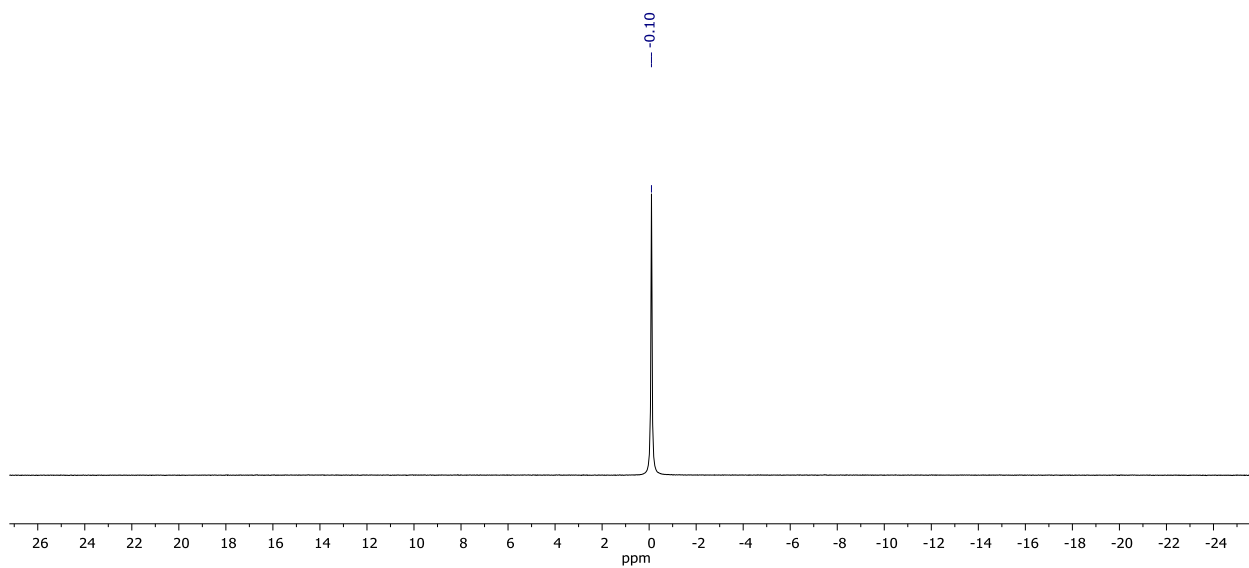
Figure S9: $^{7}Li\{^{1}H\}$ NMR spectrum (in dmso-d$_6$, 300 K, 155.47 MHz) of lithium pivalate (**4**).

Compound 5: Synthesis according to **GP2** starting from 2,2-dimethylbutyric acid (7.00 mL, 56 mmol) and *n*-butyllithium (35.00 mL, mmol, 1.6°M). Yield: quantitative (6.8 g, 56 mmol); white solid.
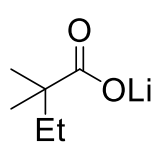
¹H NMR (400.13 MHz, dmso-d₆): δ = 1.36 (q, br, 2H, CH₂(CH₃)), 0.95 (s, 6H, CH₃), 0.74 (t, br, 3H, CH₃(CH₂)).

¹³C{¹H} NMR (125.80 MHz, dmso-d₆): δ = 182.4 (s, COO), 42.2 (s, C(CH₃)₂), 33.7 (s, CH₂C), 26.0 (s, *C*(CH₃)₂), 9.8 (s, CH₃).

⁷Li{¹H} NMR (155.47 MHz, dmso-d₆): δ = 0.03 (s, br)

Elemental analysis: calculated (%) for C₆H₁₁LiO₂: C 59.03, H 9.08, found C 58.04, H 8.96.

IR (neat): $\tilde{v}$ = 3002 (w), 2962 (m), 2932 (m), 2876 (w), 1604 (vs), 1474 (w), 1462 (m), 1397 (s), 1330 (w), 1284 (m), 1200 (w), 1186 (w), 1055 (w), 1007 (w), 933 (w), 877 (w), 803 (w), 793 (w), 764 (w), 589 (w), 562 (w), 491 (w), 451 (w) cm⁻¹.
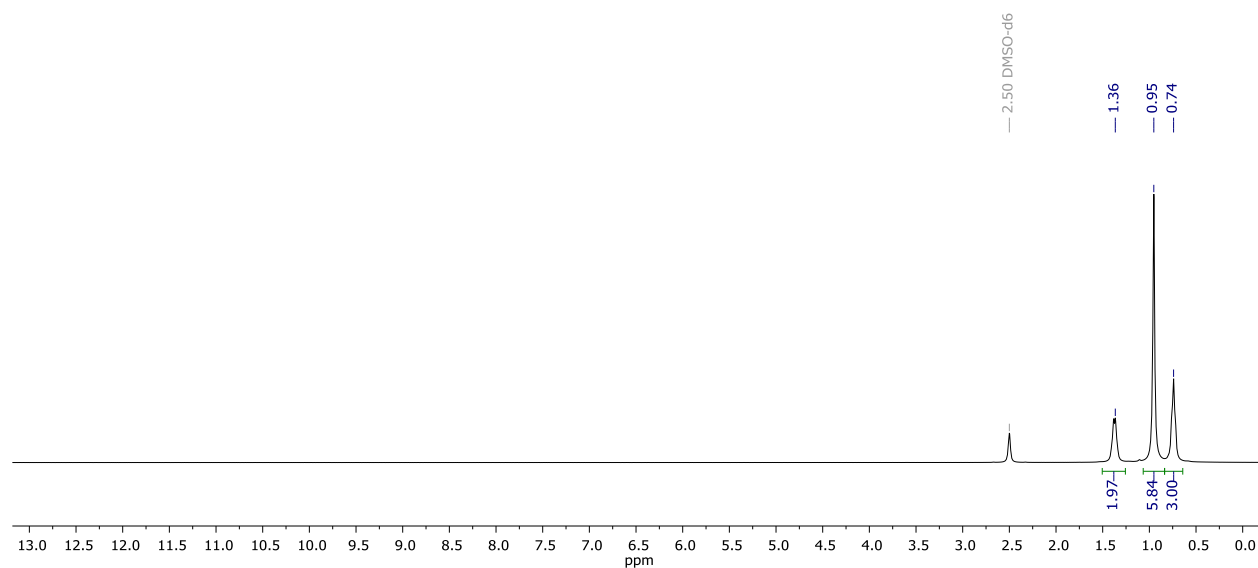
Figure S10: ¹H NMR spectrum (in dmso-d₆, 300 K, 400.13 MHz) of lithium 2,2-dimethylisobuyrate (**5**).
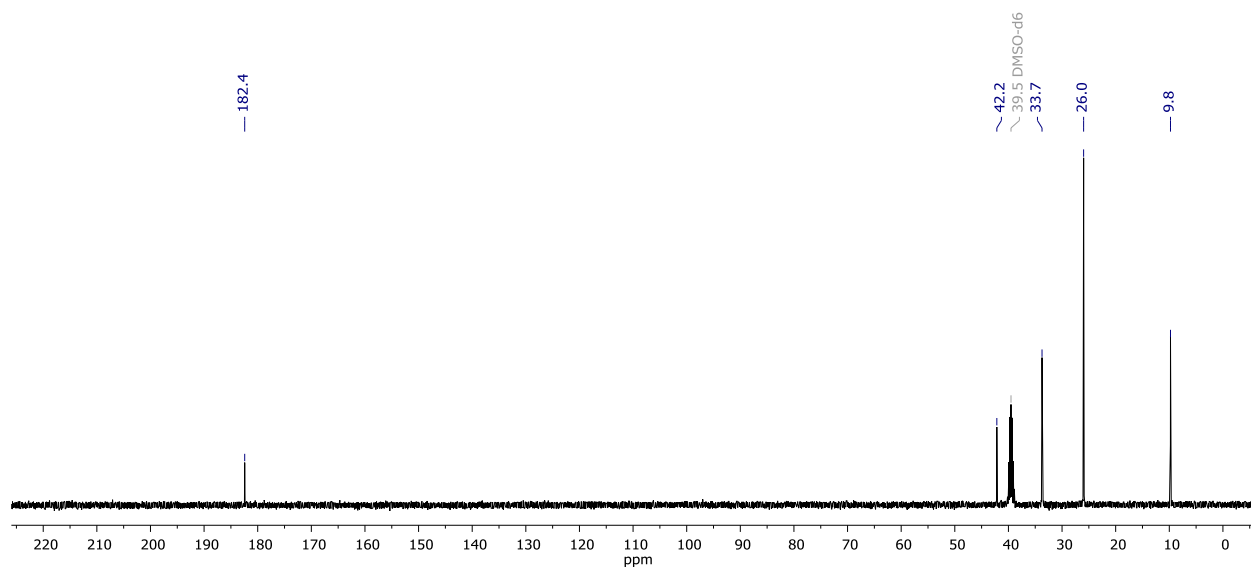
Figure S11: $^{13}C\{^{1}H\}$ NMR spectrum (in dmso-d$_6$, 300 K, 300 K, 125.80 MHz) of lithium 2,2-dimethylisobuyrate (**5**).
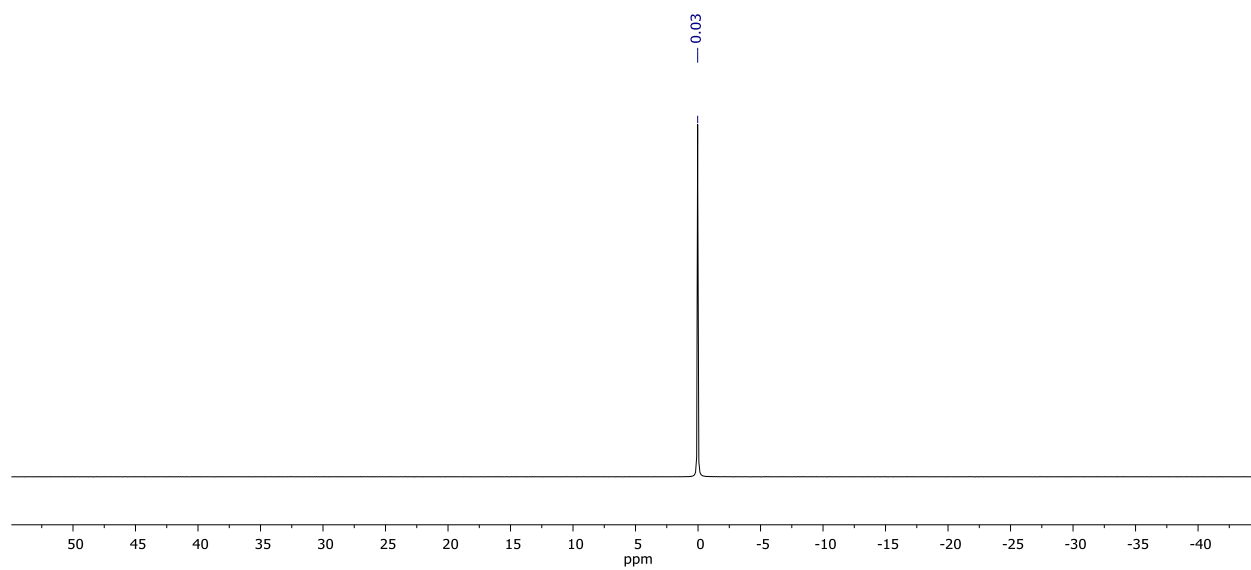
Figure S12: $^{7}Li\{^{1}H\}$ NMR spectrum (in dmso-d$_6$, 300 K, 155.47 MHz) of lithium 2,2-dimethylisobuyrate (**5**).

Compound 6: Synthesis according to **GP2** starting from 2-phenylisobutyric acid (9.20 g, 56 mmol) and *n*-butyllithium (35 mL,56 mmol, 1.6°M). Yield: quantitative (9.50 g, 56 mmol), white solid.
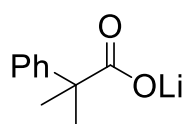
^{1}H NMR (400.13 MHz, dmso-d_6): δ = 7.38 (m, 2H, aryl-H), 7.19 (m, 2H, aryl-H),7.08 (m, 1H, aryl-H), 1.37 (s, 6H, CH$_3$).

^{13}C{^{1}H} NMR (125.80 MHz, dmso-d_6): δ = 180.1 (s, COO), 149.5 (s, *ipso*-C), 127.3 (s, aryl-C), 126.1 (s, aryl-C), 124.7 (s, aryl-C), 47.0 (s, *C*(CH$_3$)$_2$), 28.2 (s, CH$_3$).

^{7}Li{^{1}H} NMR (155.47 MHz, dmso-d_6): δ = -0.14 (s, br).

Elemental analysis: calculated (%) for C$_{10}$H$_{11}$LiO$_2$: C 70.60, H 6.52, found C 69.68, H 6.96.

IR (neat): $\tilde{v}$ = 3646 (w), 2962 (m), 2932 (m), 2876 (w), 1604 (vs), 1474 (w), 1462 (m), 1397 (s), 1362 (s), 1330 (w), 1284 (m), 1200 (w), 1186 (w), 1055 (w), 1007 (w), 933 (w), 877 (w), 803 (w), 793 (w), 764 (w), 589 (w), 562 (w), 491 (w), 451 (w) cm^{-1}.
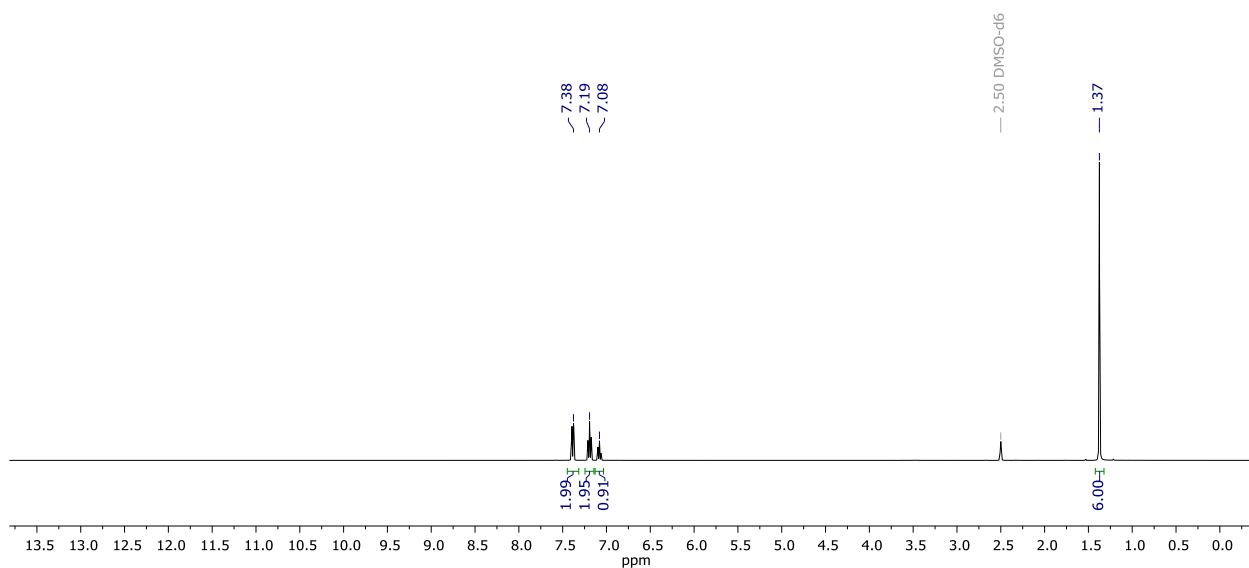
Figure S13: ^{1}H NMR spectrum (in dmso-d_6, 300 K, 400.13 MHz) of lithium 2-phenylisobutyrate (**6**).
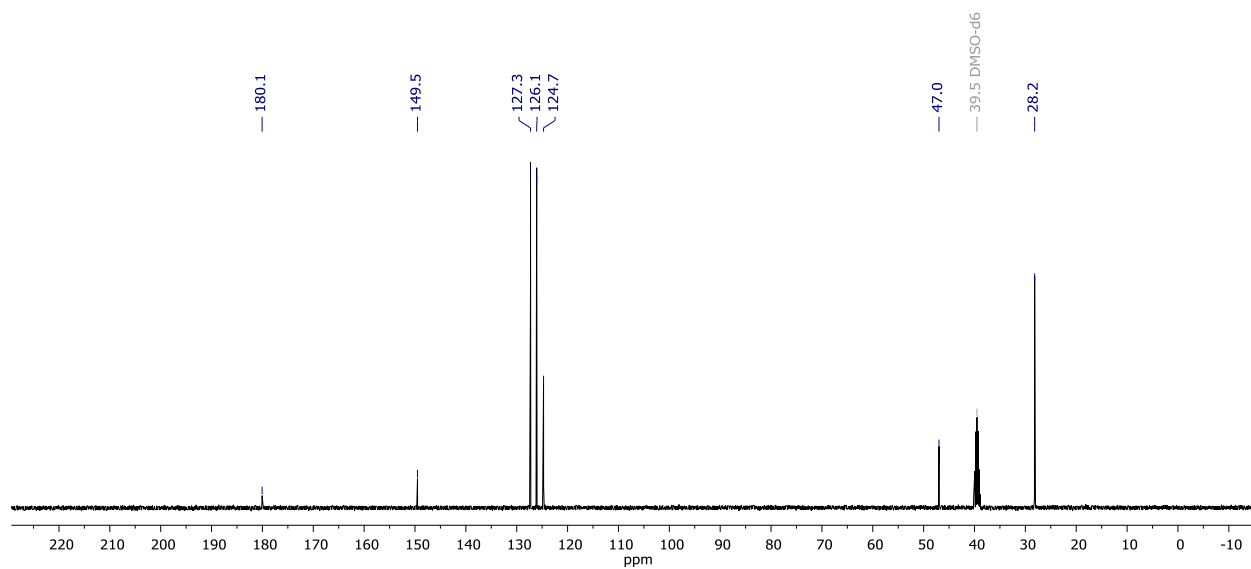
Figure S14: $^{13}C\{^1H\}$ NMR spectrum (in dmso-d_6, 300 K, 300 K, 125.80 MHz) of lithium 2-phenylisobutyrate (**6**).
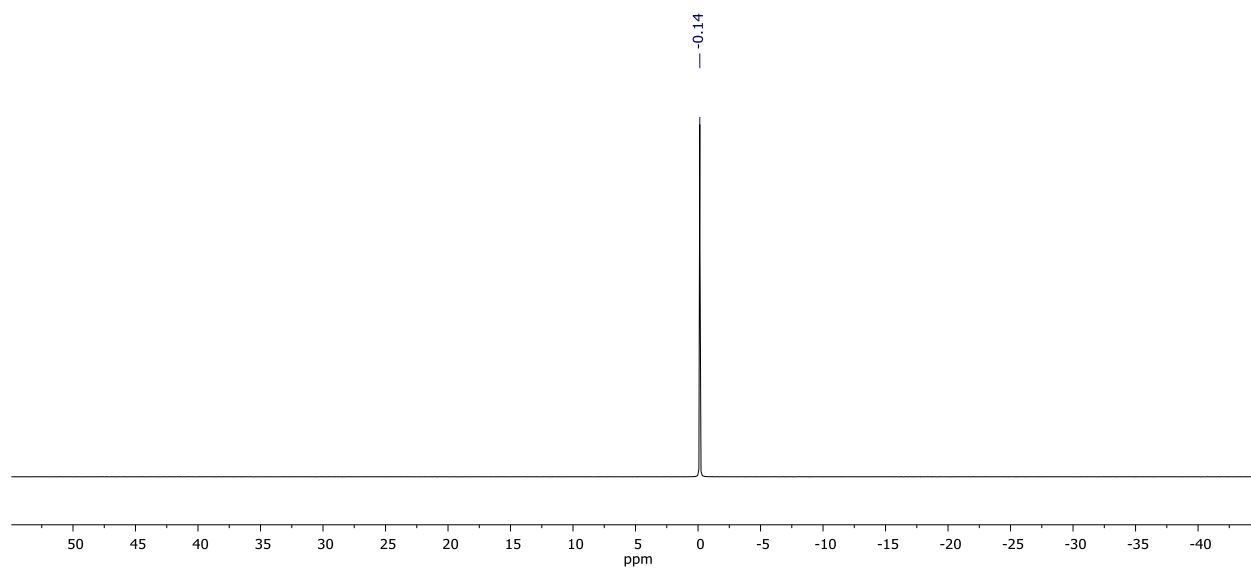
Figure S15: $^7Li\{^1H\}$ NMR spectrum (in dmso-d_6, 300 K, 155.47 MHz) of lithium 2-phenylisobutyrate (**6**).

Synthesis of multimetallic bismuth/lithium carboxylates **7-9**

General procedure (GP3): Preparation of bismuth/lithium carboxylates. A Schlenk flask was charged with bismuth(III) carboxylate (1.00 eq.) and lithium carboxylate (2.00 eq.). Anhydrous acetonitrile (10 mL) was added and the reaction mixture was heated to reflux until a clear solution was obtained. The reaction mixture was allowed to cool to room temperature. Already overnight single crystals of the heterobimetallic complex were formed in high yields. The crystalline material was isolated by filtration, washed first with the mother liquor and then once with 3 mL of diethyl ether. The resulting white crystalline solid was dried in a stream of argon. The coordinated acetonitrile is readily removed under vacuum, which explains the low values for N in the elemental analysis of complexes **7-9**. Note that the heterobimetallic bismuth/lithium carboxylates **7-9** were also obtained using wet acetonitrile.

Compound 7: Synthesis according to **GP3** starting from bismuth pivalate (**1**) (205 mg, 0.40 mmol) and lithium pivalate (**4**) (86 mg, 0.80 mmol). Yield: 95.5 % (294 mg, 0.192 mmol), white crystalline solid.

$Bi_2Li_4(O_2CR)_{10}(MeCN)_2$

$O_2CR =$

^{1}H NMR (400.13 MHz, CD_2Cl_2): $\delta = = = 1.98$ (s, 5.3H, CH_3CN), 1.17 (s, br, 90H, CH_3).

^{13}C{^{1}H} NMR (100.62 MHz, CD_2Cl_2): $\delta = 189.7$ (br, RCOO), 117.2 (CN), 41.7 (C(CH_3)$_3$), 27.9 (CH_3), 2.2 (CH_3(CN)).
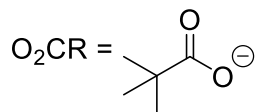
^{7}Li{^{1}H} NMR (155.47 MHz, CD_2Cl_2): $\delta = -0.10$ (s, br).

HRMS (ESI): m/z calculated for [$C_{54}H_{96}Bi_2Li_4N_2O_{20}$] (M)$^+$ 1534.6769, found 237.1377 (237.1400) [Li_2L_2+Na]$^+$, 391.1392 (391.0382) [$BiL_1+MeCN+K$]$^+$, 535.1505 (535.1504) [BiL_3+Na]$^+$, 659.2009 (658.1997) [$BiLiL_4+K$]$^+$.

Elemental analysis: calculated (%) for $C_{54}H_{96}Bi_2Li_4N_2O_{20}$: C 42.14, H 6.29, N 1.82, found C 41.94, H 6.24, N 1.33.

IR (neat): $\tilde{v} = 2959$ (s), 2929 (m), 2904 (m), 2870 (m), 2302 (w), 2272 (w), 1582 (s), 1570 (s), 1536 (s), 1481 (s), 1409 (vs), 1360 (s), 1031 (w), 935 (w), 903 (m), 797 (m), 597 (m), 551 (m) cm^{-1}.
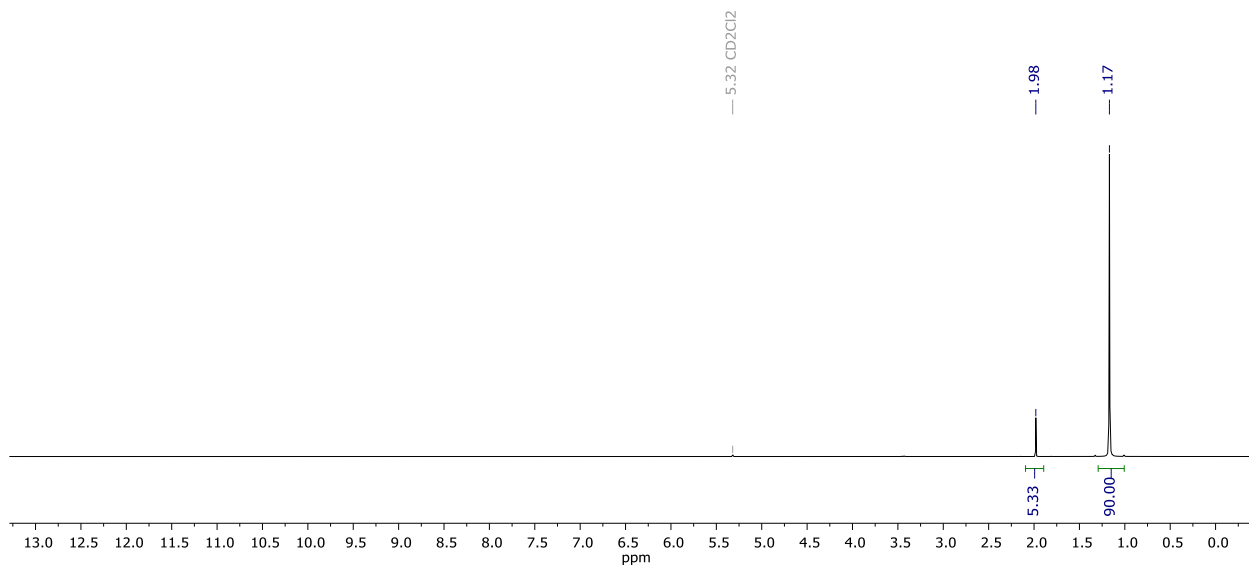
Figure S16: ^{1}H NMR spectrum (in CD_2Cl_2, 300 K, 400.13 MHz) of compound (**7**).
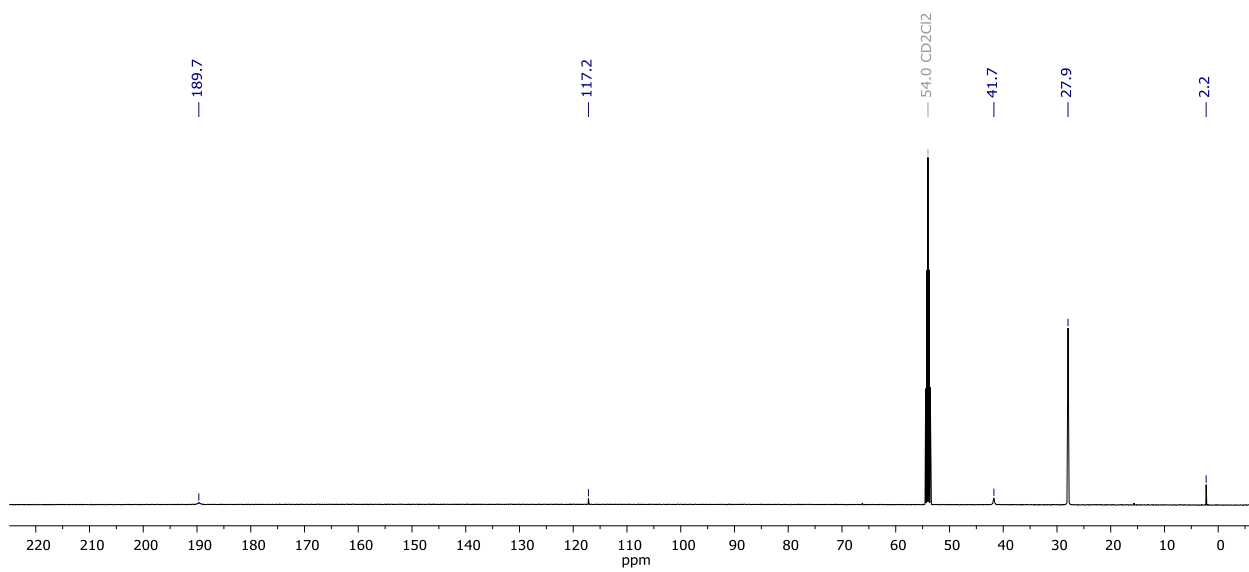
Figure S17: $^{13}C\{^1H\}$ NMR spectrum (in CD_2Cl_2, 300 K, 300 K, 100.62 MHz) of compound (**7**).
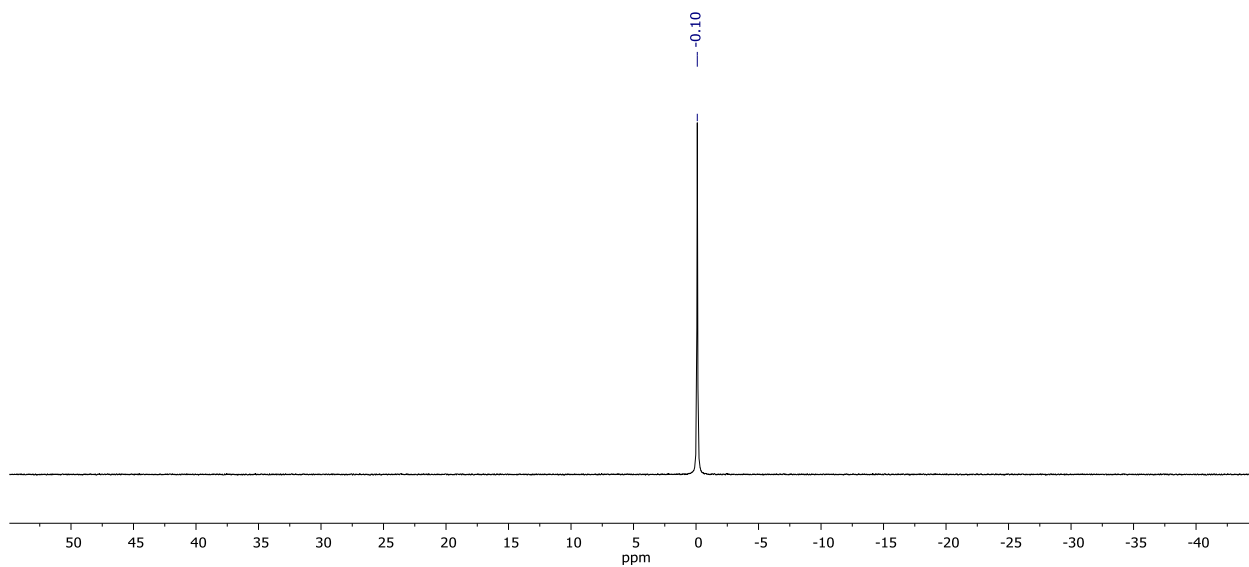
Figure S18: ^{7}Li{^{1}H} NMR spectrum (in CD$_2$Cl$_2$, 300 K, 155.47 MHz) of compound (**7**).
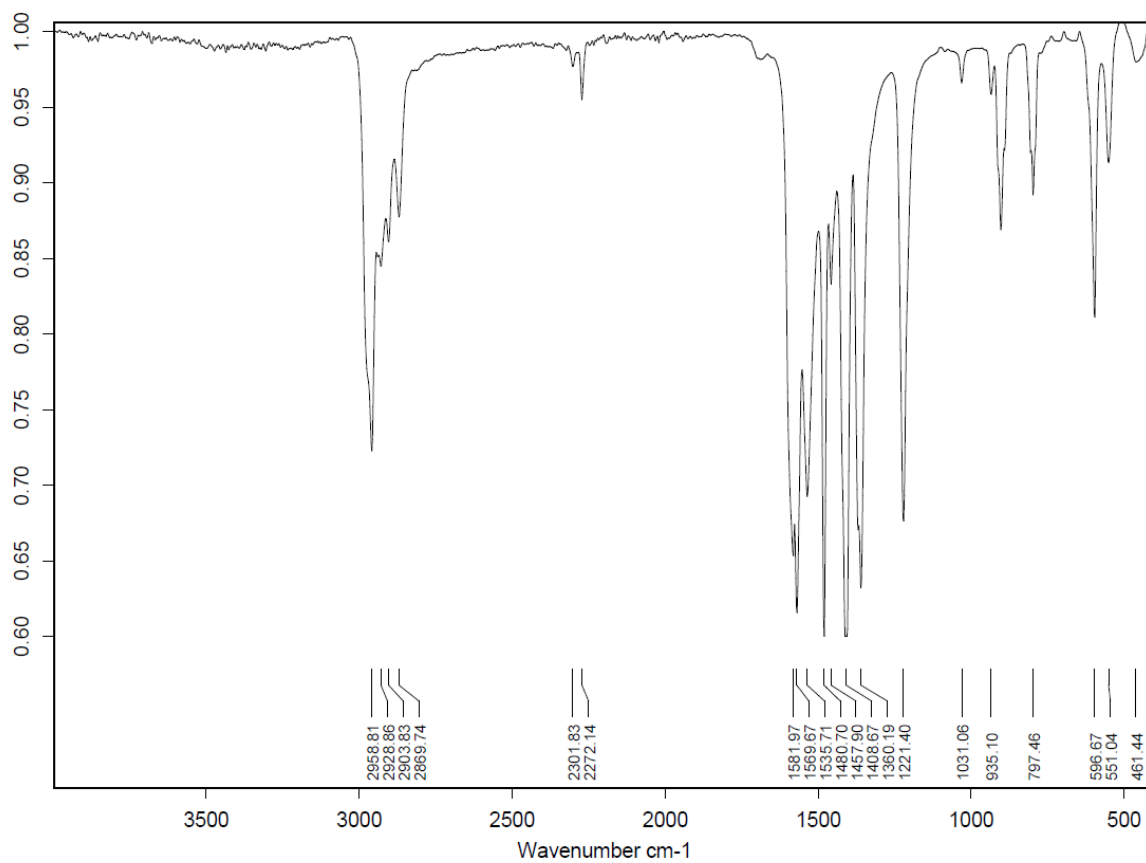
Figure S19: Infrared spectrum of compound (**7**).

Li(piv)

Bi(piv)₃

Bi(piv)₃ + 1eq. Li(piv)

Bi(piv)₃ + 2eq. Li(piv)
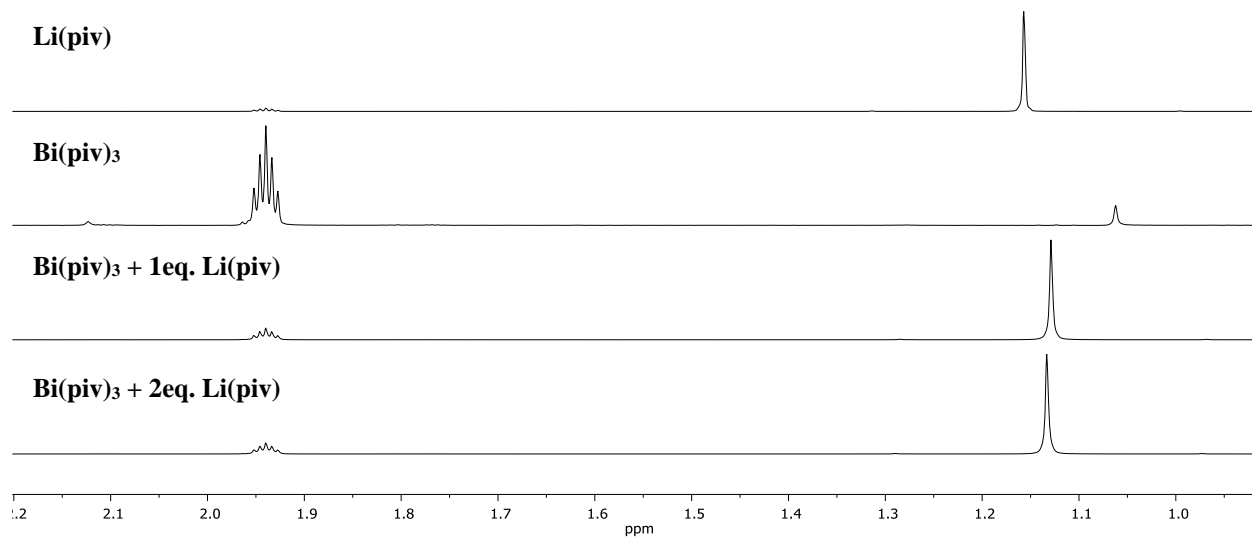
***Figure S20*:** Stacked ¹H NMR spectra (in MeCN-d₃, 300 K, 400.13 MHz) of mixing experiments with pivalate as ligand.

Li(piv)

Bi(piv)₃ + 1eq. Li(piv)

Bi(piv)₃ + 2eq. Li(piv)
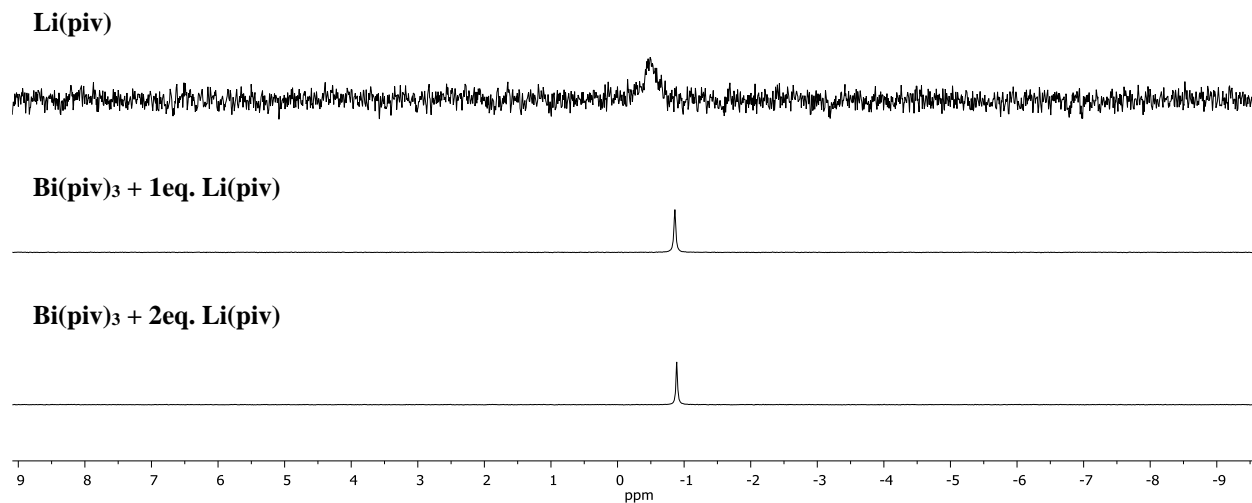
***Figure S21*:** Stacked ⁷Li{¹H} NMR spectrum (in MeCN-d₃, 300 K, 155.47 MHz) of mixing experiments with pivalate as ligand.

Compound 8: Synthesis according to **GP3** starting from bismuth 2,2-dimethylbutyrate (**2**) (222 mg, 0.40 mmol) and lithium 2,2-dimethylbutyrate (**5**) (98 mg, 0.80 mmol). Yield: 91.1 % (306 mg, 0.182 mmol), white crystalline solid.

$Bi_2Li_4(O_2CR)_{10}(MeCN)_2$

$O_2CR =$

¹H NMR (400.13 MHz, CD_2Cl_2): δ = 1.98 (s, 7H, CH_3CN), 1.55 (q, br, $^3J_{HH}$ = 7.4 Hz, 20H, $CH_2(CH_3)$), 1.12 (s, br, 60H, CH_3), 0.86 (t, br, $^3J_{HH}$ = 7.5 Hz, 30H, $CH_3(CH_2)$).

¹³C{¹H} NMR (100.62 MHz, CD_2Cl_2): δ = δ = 189.7 (br, RCOO), 117.1 (CN), 45.9 ($C(CH_3)_2$), 34.1 (CH_2C), 25.3 (($CH_3)_2C$), 9.8 (CH_3), 2.2 ($CH_3(CN)$).

⁷Li{¹H} NMR (155.47 MHz, CD_2Cl_2): δ = 0.06 (s, br), -0.52 (s, br)

HRMS (ESI): m/z calculated for $[C_{64}H_{116}Bi_2Li_4N_2O_{20}]$ (M)$^+$ 1678.8369, found 561.22385 (561.2305) $[BiL_3+H+Li]^+$, 577.1974 (577.1973) $[BiL_3+Na]^+$, 699.2897 (699.2962) $[BiLiL_4+H+Na]^+$, 715.2635 (715.2701) $[BiLiL_4+H+K]^+$.

Elemental analysis: calculated (%) for $C_{64}H_{116}Bi_2Li_4N_2O_{20}$: C 45.77, H 6.96, N 1.67, found C 44.25, H 6.98, N 0.15.

IR (neat): $\tilde{v}$ = 3482 (br, w), 2966 (vs), 2928 (s), 2880 (m), 2303 (w), 2273 (w), 1690 (w), 1572 (vs), 1531 (s), 1475 (s), 1461 (m), 1399 (vs), 1370 (s), 1357 (s), 1286 (w), 1203 (m), 1063 (w), 1052 (w), 1008 (w), 934 (w), 886 (w), 804 (w), 793 (w), 765 (w), 633 (w), 585 (w), 549 (w), 459 (w) cm^{-1}.
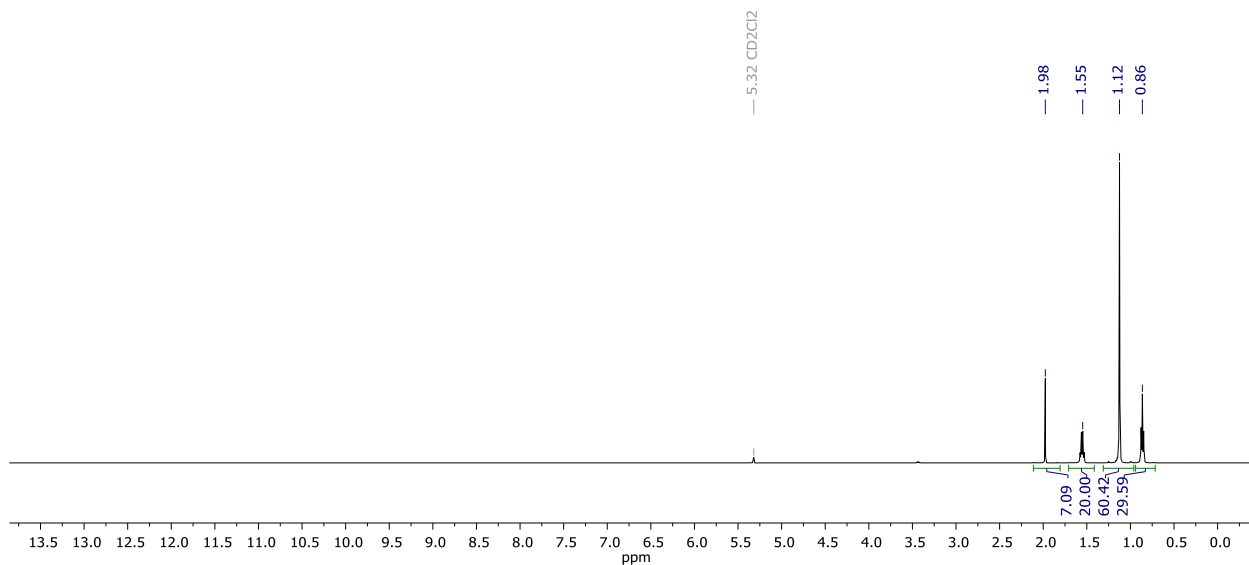
Figure S22: ¹H NMR spectrum (in CD_2Cl_2, 300 K, 400.13 MHz) of compound (**8**).
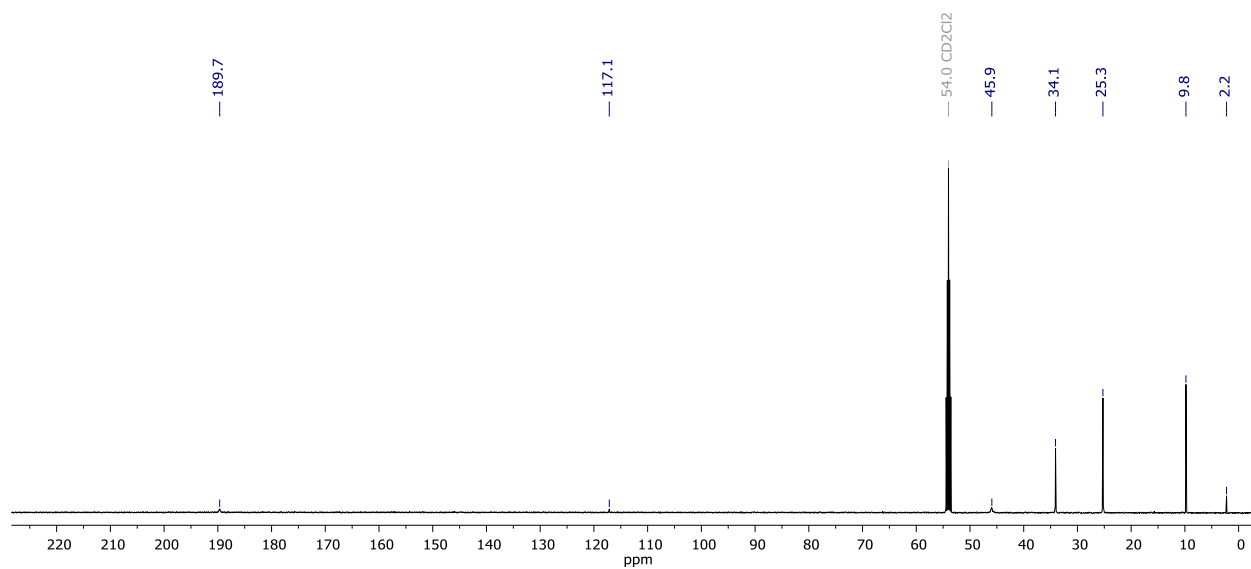
Figure S23: $^{13}C\{^1H\}$ NMR spectrum (in CD_2Cl_2, 300 K, 300 K, 100.62 MHz) of compound (**8**).
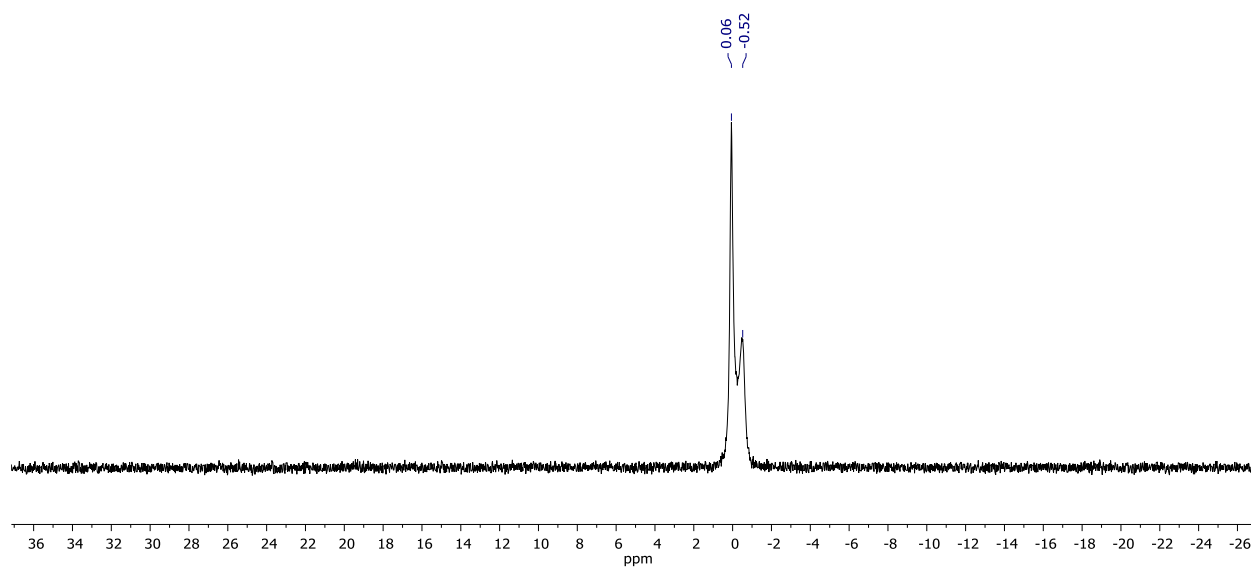
Figure S24: $^7Li\{^1H\}$ NMR spectrum (in CD_2Cl_2, 300 K, 155.47 MHz) of compound (**8**).
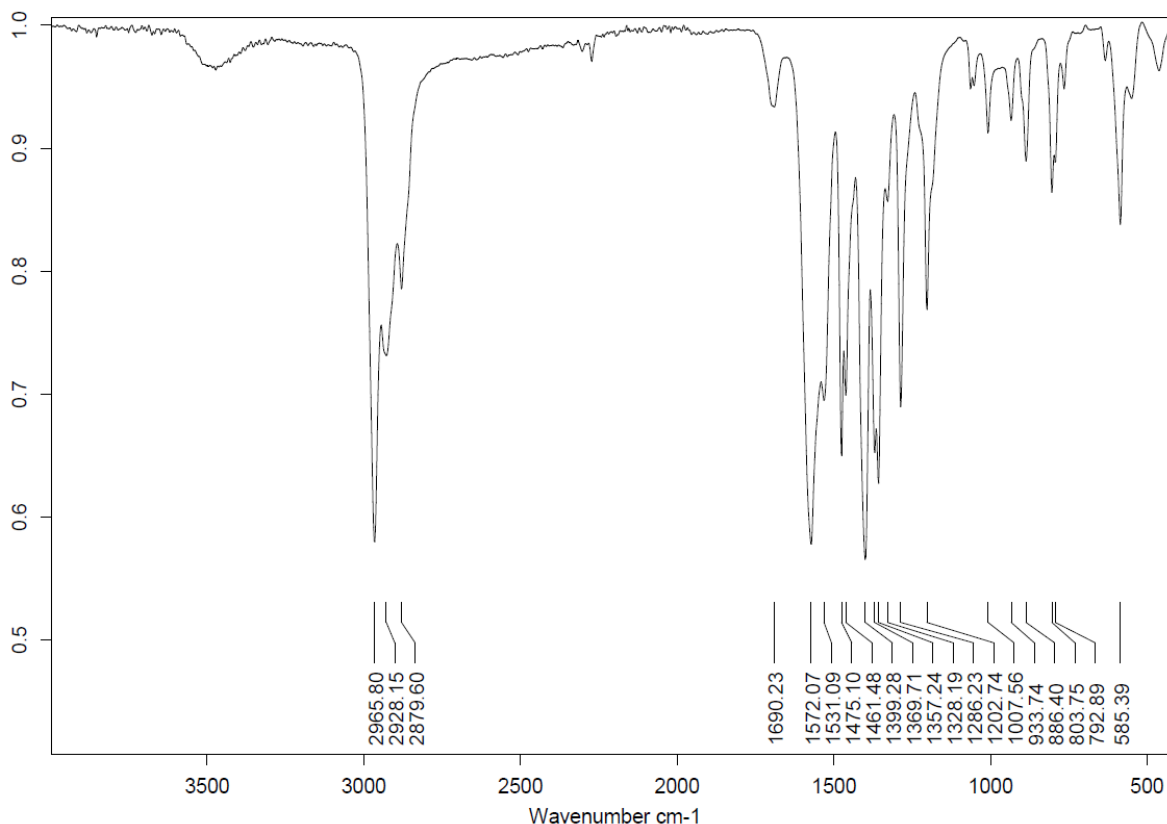
Figure S25: Infrared spectrum of compound (**8**).

Compound 9: Synthesis according to **GP3** starting from bismuth 2-phenylisobutyrate (**3**) (279 mg, 0.40 mmol) and lithium 2-phenylisobutyrate (**6**) (136 mg, 0.80 mmol). Yield: 92 % (396 mg, 0.184 mmol), white crystalline solid.

$Bi_2Li_4(O_2CR_{10}(MeCN)_2$

$O_2CR =$ Ph

^{1}H NMR (400.13 MHz, CD_2Cl_2): $\delta = 7.27$ (m, 50H, aryl-H), 1.97 (s, 6H, CH_3CN), 1.39 (s, br, 60H, CH_3)
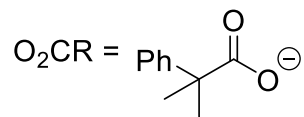
^{13}C{^{1}H} NMR (100.62 MHz, CD_2Cl_2): $\delta = 187.5$ (br, RCOO), 146.4 (*ipso*-C), 128.8 (aryl-C), 127.0 (aryl-C), 126.6 (aryl-C), 49.8 (C($CH_3)_2$), 27.3 (CH_3), 2.2 (CH_3(CN)).

^{7}Li{^{1}H} NMR (155.47 MHz, CD_2Cl_2): $\delta = -013$ (s, br), -1.47 (s, br).

HRMS (ESI): m/z calculated for $[C_{104}H_{116}Bi_2Li_4N_2O_{20}]$ (M)$^+$ 2158.8369, found 721.1979 (721.1973) $[BiL_3+Na]^+$, 891.2899 (891.2962) $[BiLiL_4+H+Na]^+$, 907.2637 (907.2701) $[BiLiL_4+H+K]^+$, 1061.3823 (1061.3950) $[BiLi_2L_5+2H+Na]^+$, 1093.3295 (1093.2537) $[Bi_2L_4+Na]^+$, 1403.4340 (1402.4308) $[Bi_2LiL_6]^+$, 1589.4997 (1589.5043) $[Bi_2LiL_7+H+Na]^+$.

Elemental analysis: calculated (%) for $C_{104}H_{116}Bi_2Li_4N_2O_{20}$: C 57.84, H 5.41, N 1.30, found C 56.84, H 5.44, N 0.69.

IR (neat): $\tilde{v}$ = 3501 (br,w), 3088 (w), 3059 (w), 3025 (w), 2966 (m), 2930 (m), 2873 (w), 2310 (w), 2279 (w), 1697 (w), 1575 (vs), 1544 (s), 1496 (m), 1472 (m), 1446 (m), 1395 (vs), 1357 (vs), 1285 (w), 1252 (w), 1183 (m), 1103 (w), 1107 (w), 1030 (w), 947 (w), 878 (w), 796 (w), 768 (w), 751 (w), 733 (w), 696 (m), 639 (m), 567 (w) cm^{-1}.
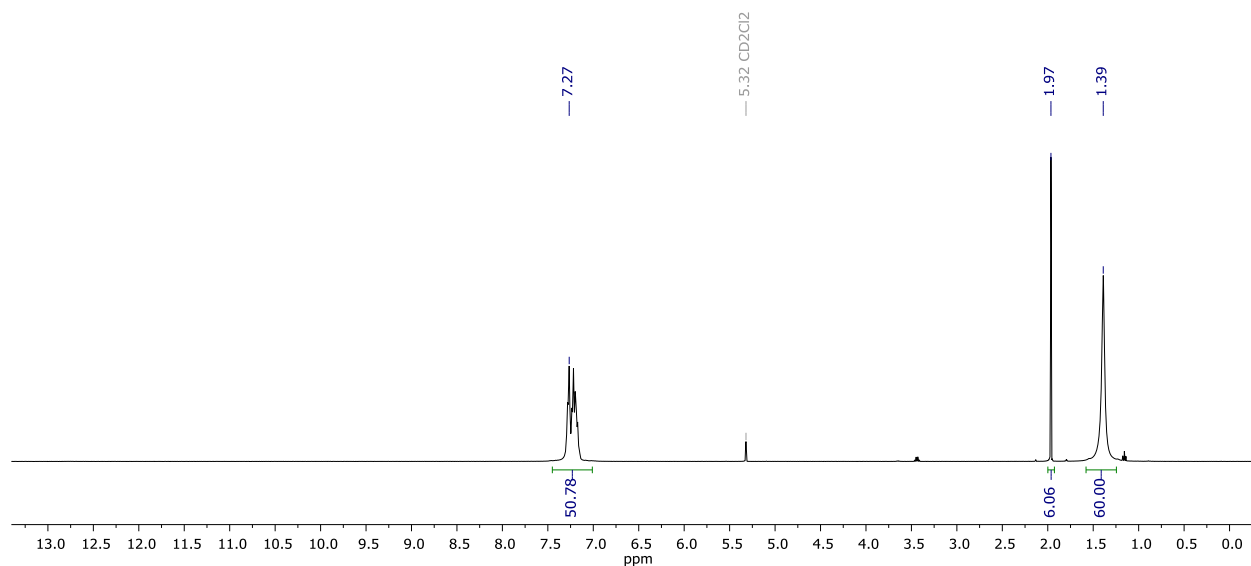
Figure S26: ^{1}H NMR spectrum (in CD$_2$Cl$_2$, 300 K, 400.13 MHz) of compound (**9**).
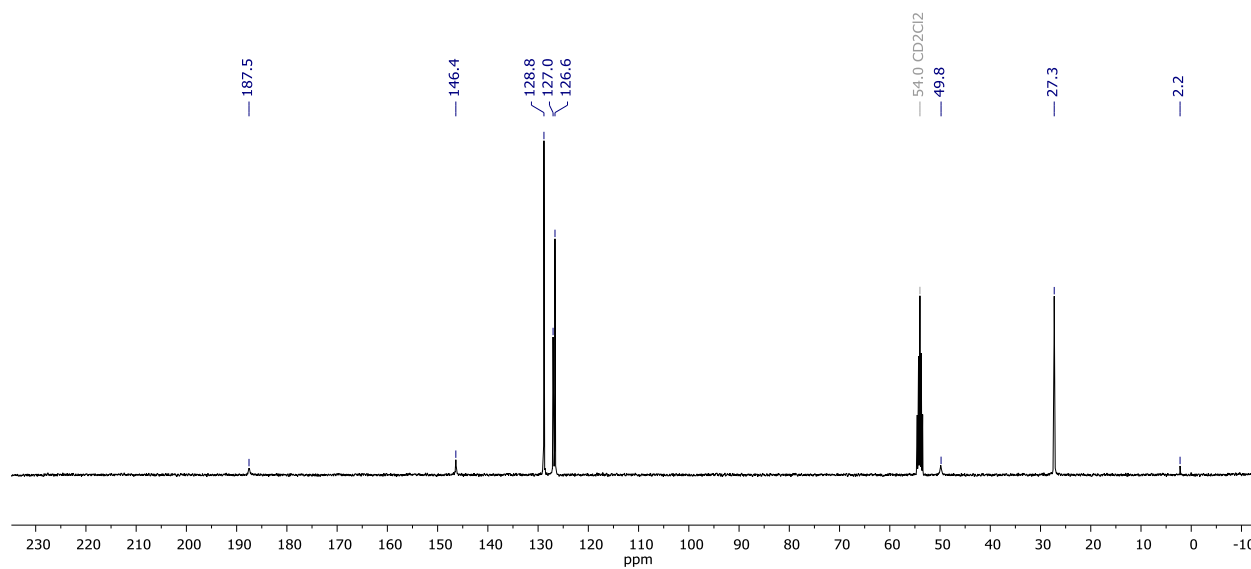
Figure S27: ^{13}C{^{1}H} NMR spectrum (in CD$_2$Cl$_2$, 300 K, 300 K, 100.62 MHz) of compound (**9**).

— 21 —
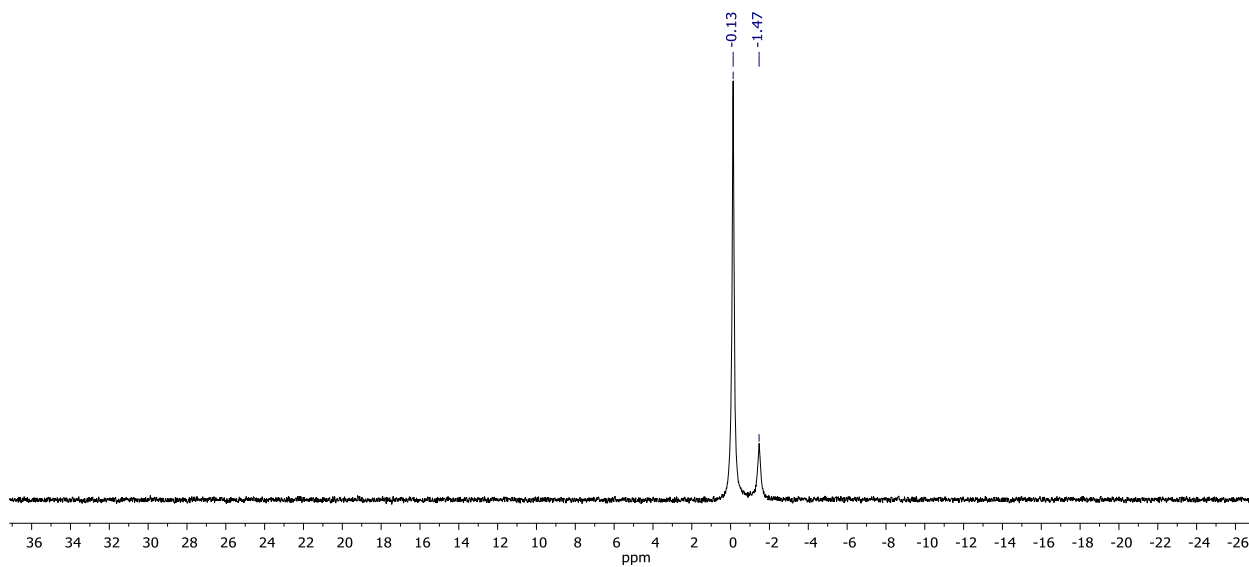
Figure S28: ^{7}Li{^{1}H} NMR spectrum (in CD_2Cl_2, 300 K, 155.47 MHz) of compound (**9**).
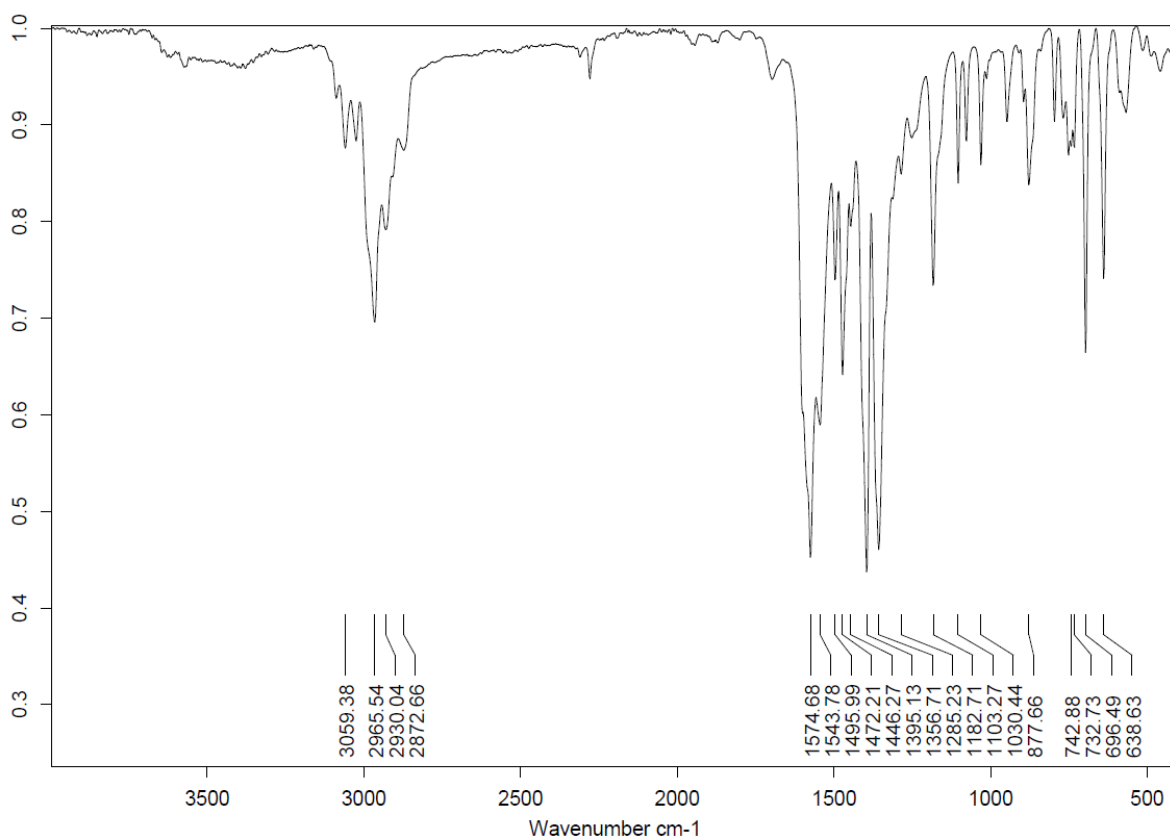
Figure S29: Infrared spectrum of compound (**9**).

Low temperature NMR Studies
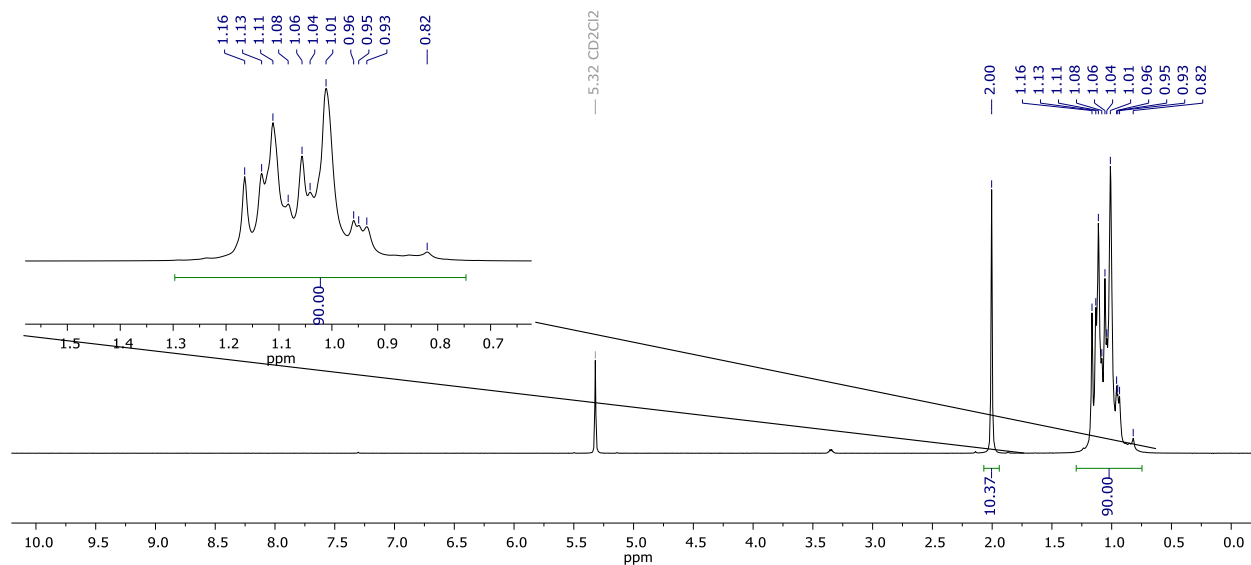
Figure S30: ^{1}H NMR spectrum (in CD$_2$Cl$_2$, 193 K, 499.83 MHz) of compound (**7**).
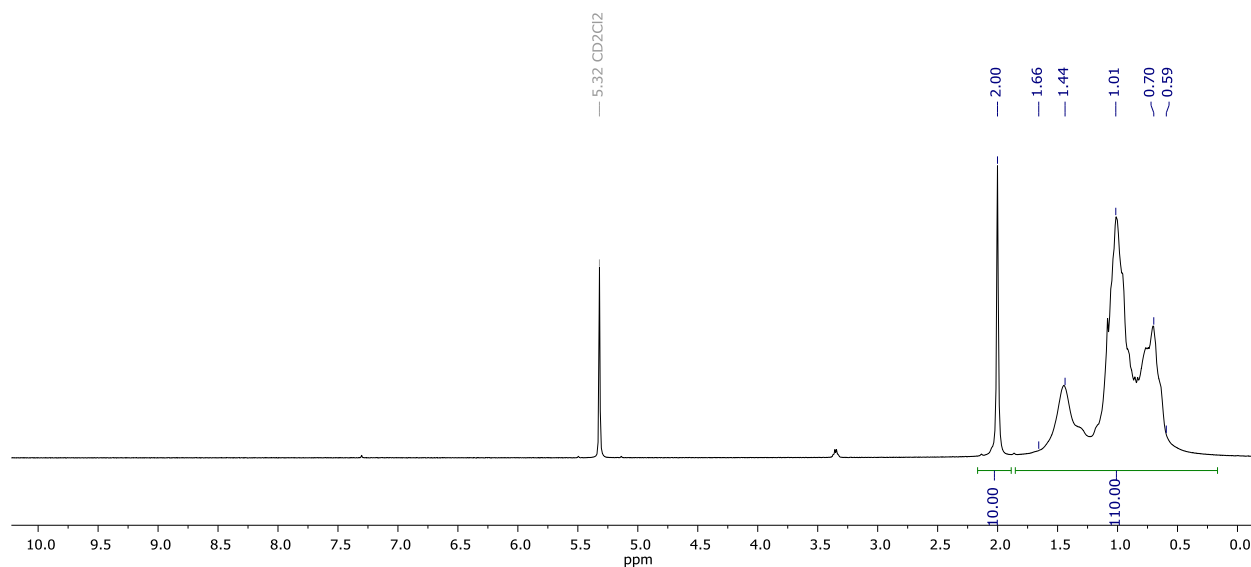
Figure S31: ^{1}H NMR spectrum (in CD$_2$Cl$_2$, 193 K, 499.83 MHz) of compound (**8**).

— 23 —
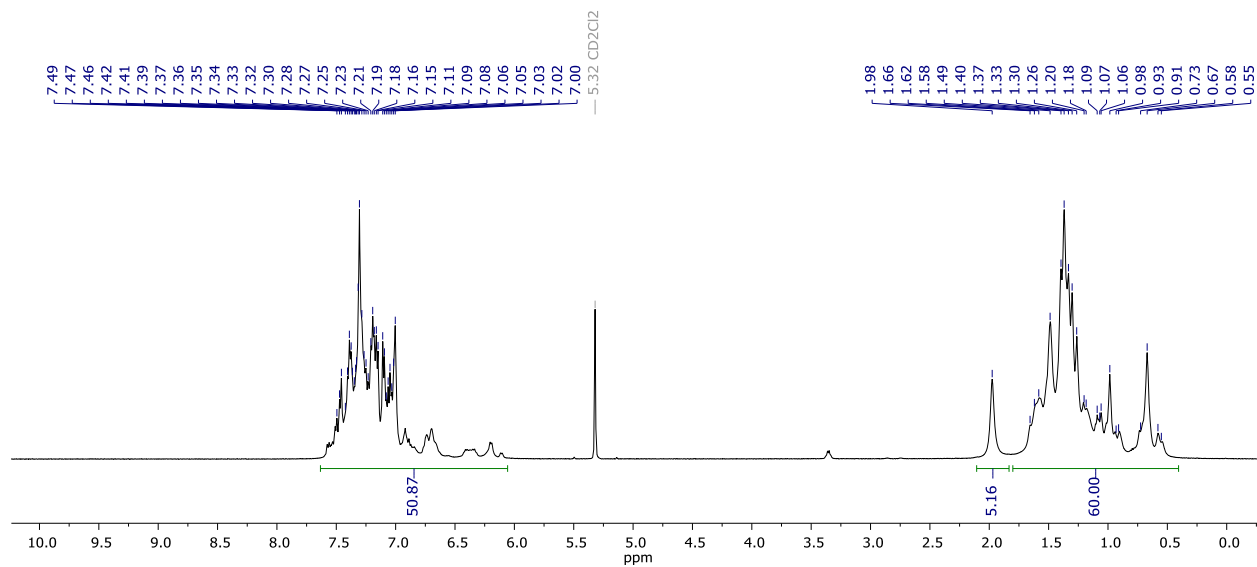
Figure S32: ^{1}H NMR spectrum (in CD_2Cl_2, 193 K, 499.83 MHz) of compound (**9**).

Reactivity with Isocyanate and Alcohol
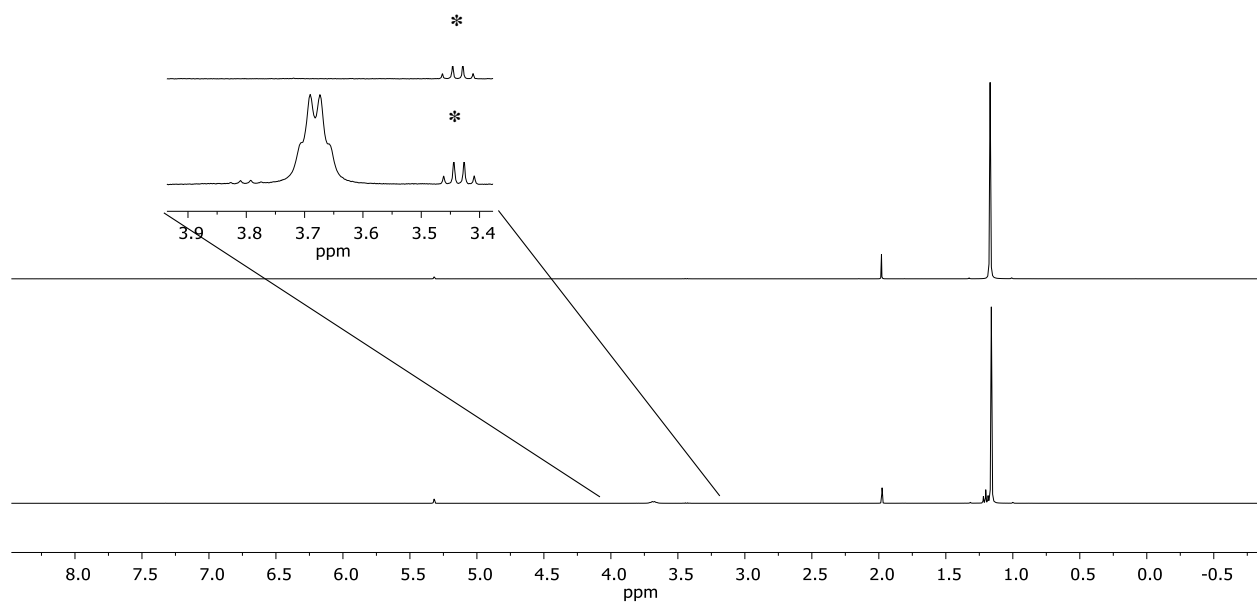
Figure S33: Stacked ^{1}H NMR spectra (in CD_2Cl_2, 300 K, 400.13 MHz) of compound **7** (top) and stoichiometric mixture of **7** with absolute EtOH (bottom), Acetonitril is highfield shifted. *Diethylether impurity.
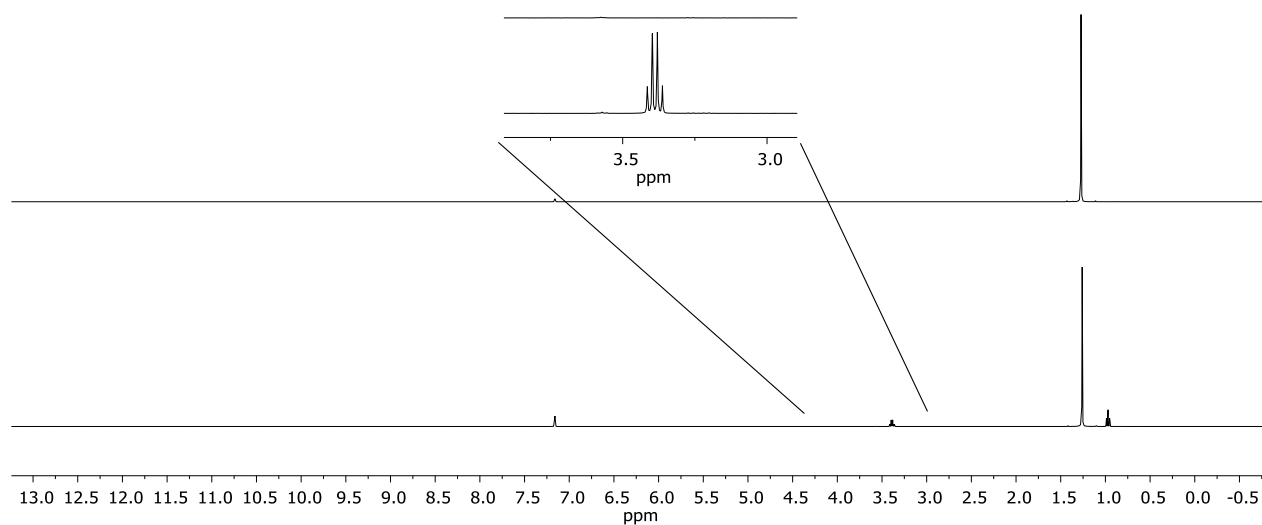
Figure S34: Stacked ^{1}H NMR spectra (in C_6D_6, 300 K, 400.13 MHz) of compound **1** (top) and stoichiometric mixture of **1** with absolute EtOH (bottom).
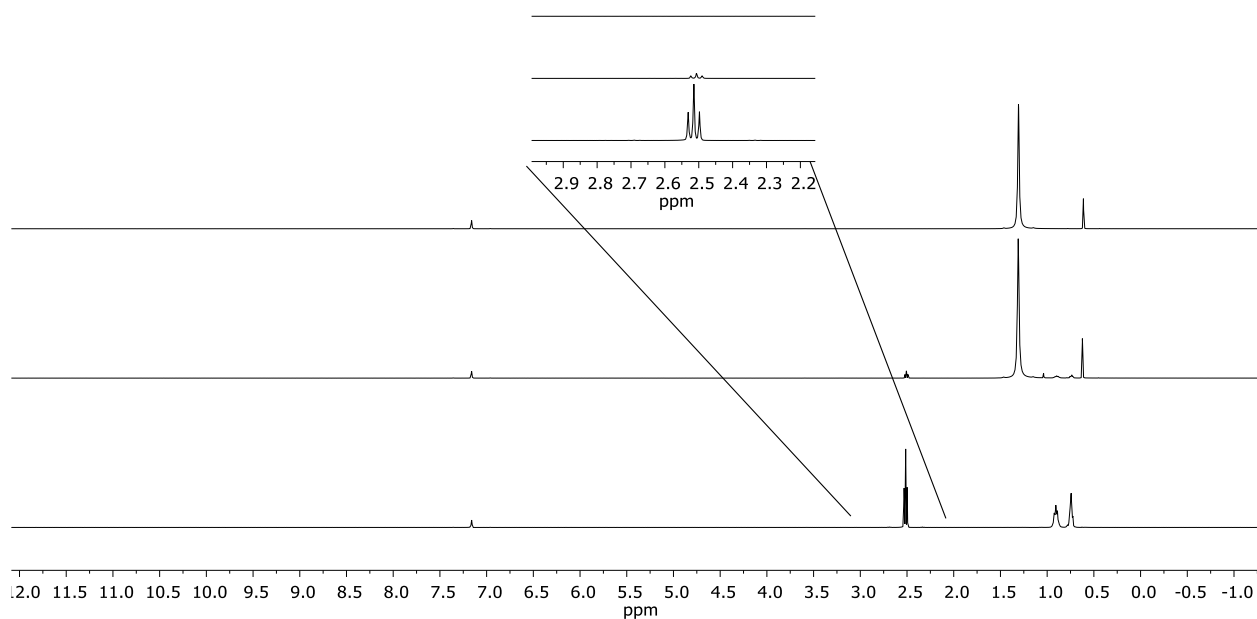
Figure S35: Stacked ^{1}H NMR spectra (in C_6D_6, 300 K, 400.13 MHz) of compound **7** (top), of a stoichiometric mixture of **7** and 1,6-hexamethylene diisocyanate (middle), and of 1,6-hexamethylene diisocyanate (bottom).
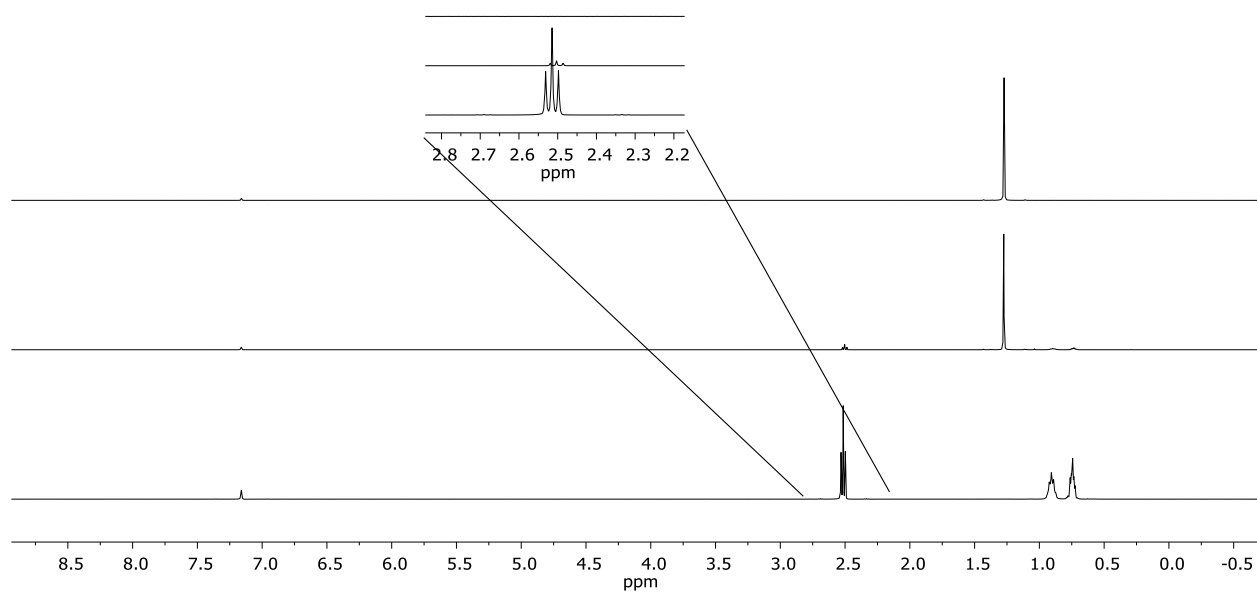
Figure S36: Stacked ^{1}H NMR spectra (in C_6D_6, 300 K, 400.13 MHz) of compound **1** (top), of a stoichiometric mixture of **1** and 1,6-hexamethylene diisocyanate (middle), and of 1,6-hexamethylene diisocyanate (bottom).

DOSY-NMR Study

^{1}H DOSY NMR experiments were carried out with approximately 0.05 M solutions of compound **1** and **7** in the presence of the internal standard tetramethylsilane (TMS) in MeOD at 300 K. The diffusion ordered NMR measurements were performed on Agilent DD2 500 MHz using the pulse program Doneshot[3] with typical acquisition parameters gradient pulse duration (δ) = 2.5 ms and timescale of the diffusion measurement (Δ) = 50 ms. Assuming a spherical size of the molecule the diffusion coefficient D is given by the Stokes-Einstein equation[4] (**E1**)

Equation E1 $\qquad D = \dfrac{k_b T}{6\pi\eta r_H}$

where k_B is the Boltzmann constant, T is the temperature, η is the viscosity of the solvent and r_H the hydrodynamic radius. Considering the diffusion coefficient D and the hydrodynamic radius of TMS, the hydrodynamic radii of compounds **1** and **7** can be calculated with equation **E2**

Equation E2 $\qquad \dfrac{D_{TMS}}{D_x} = \dfrac{r_x}{r_{TMS}}$

where D_{TMS} is the diffusion coefficient of TMS, r_{TMS} the hydrodynamic radius of TMS (calculated by hard-sphere-increments[5]), D_x the measured diffusion coefficient of compound x and r_x the desired value for compound x.
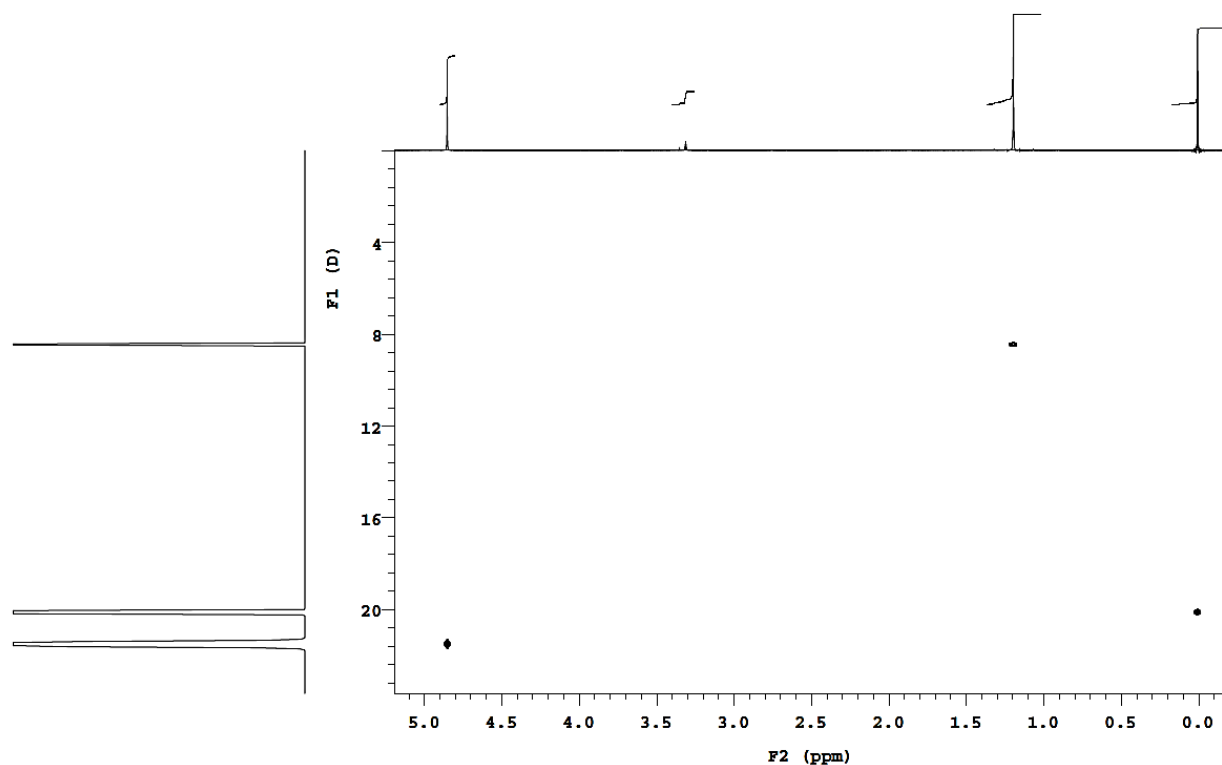
Figure S37: ^{1}H DOSY NMR spectrum of compound **1** at 300 K in MeOD.
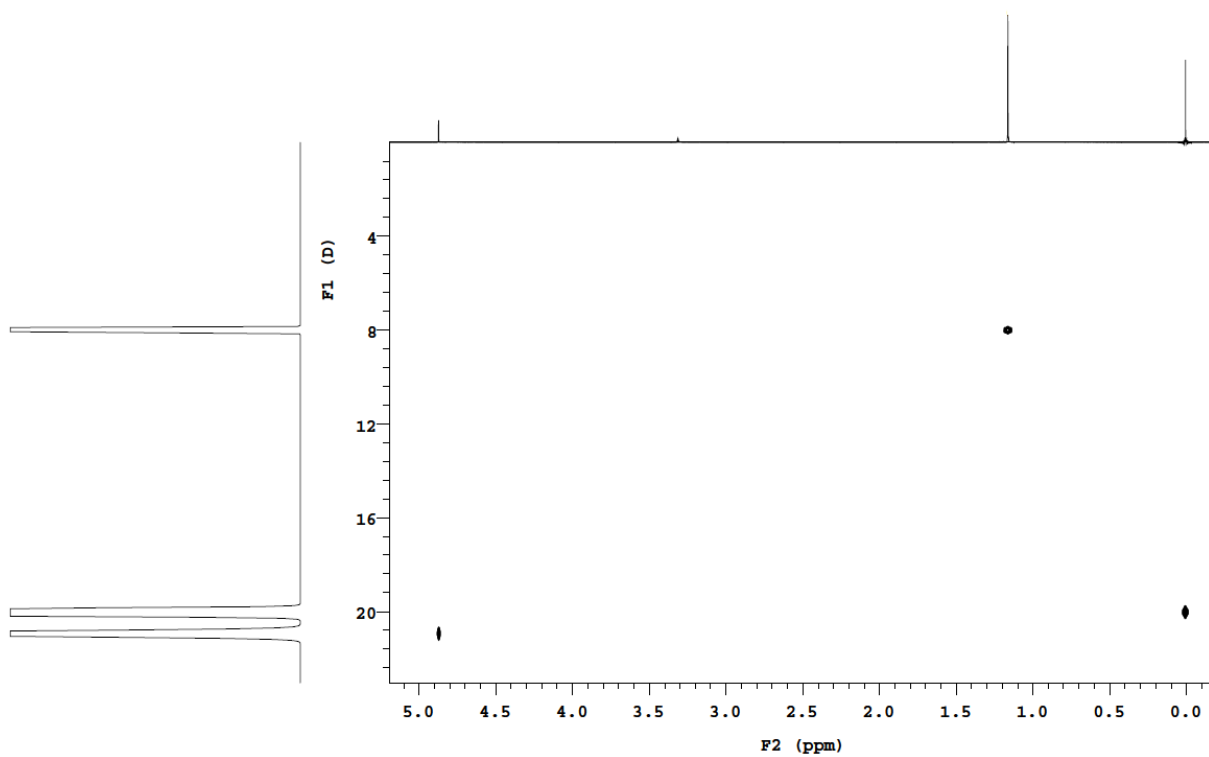
Figure S38: ^{1}H DOSY NMR spectrum of compound **7** at 300 K in MeOD.

Table S1: Hydrodynamic radius r_H from ^{1}H-DOSY-NMR and averaged radius from the crystal structure of Bi(piv)$_3$ (**1**) and heterobimetallic complex **7** in [Å]

Entry	Bi(piv)$_3$ (**1**)	Bi$_2$Li$_4$(piv)$_{10}$(MeCN)$_2$ (**7**)
averaged solid-state radius	7.96[a]	8.58
hydrodynamic radius r_H	7.64[b]	8.04[b]

[a] Calculated from Literature crystal structure.[6] [b] Recorded in MeOD.

The averaged solid-state radius of compound 1 and 7 where determined based on the crystal structure with the software Diamond (version 4).

Urethane reaction - Catalysis and kinetics

The catalyst activity was analyzed using the following urethane-forming model reaction: To a solution of 11 mmol of 2-ethylhexyl-(6-isocyanatohexyl)-carbamates (commercially available as Desmodur LD (3.3 mL)), 11 mmol of absolute ethanol (0.65 mL) and 2.2 mL of xylene was added 0.05 mol% catalyst (based on the amount of bismuth) at room temperature. Catalysts **7-9** were freshly prepared before being used for catalysis.

The isocyanate conversion and thus the formation of a urethane group are investigated by horizontal ATR-IR spectroscopy. For this purpose, an aliquot of 0.05 mL is taken from the reaction mixture at defined time intervals and analyzed directly by IR spectroscopy. The relative intensity decrease of the asymmetric isocyanate stretching band at 2260 cm^{-1} was used to determine the conversion. The initial free isocyanate content of the reaction mixture was determined at room temperature in the absence of a catalyst. All IR spectra were normalized to the bands of the symmetrical and asymmetrical stretching vibrations of the CH$_2$ groups (3000 – 2870 cm^{-1}).
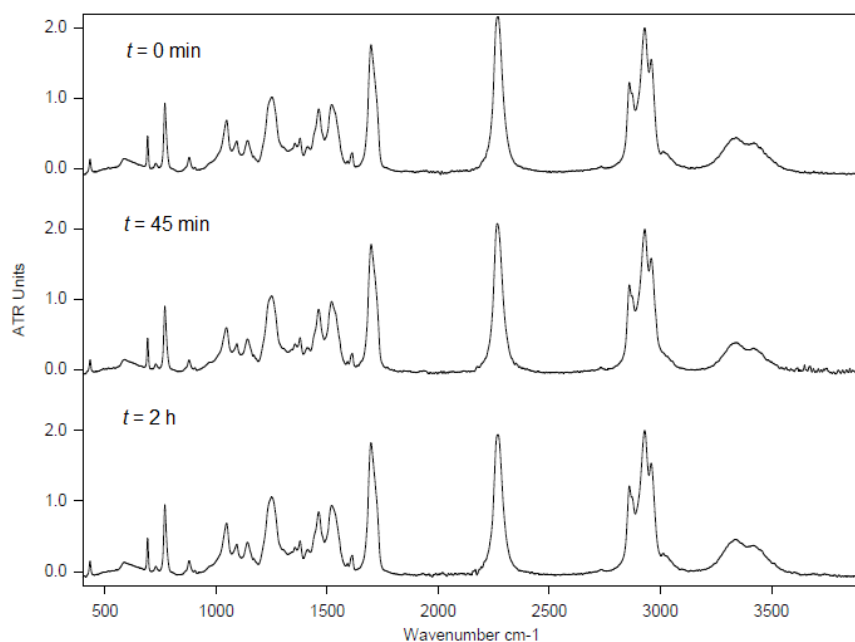
Figure S39: Urethane formation by reaction of Desmodur LD and ethanol without catalyst.
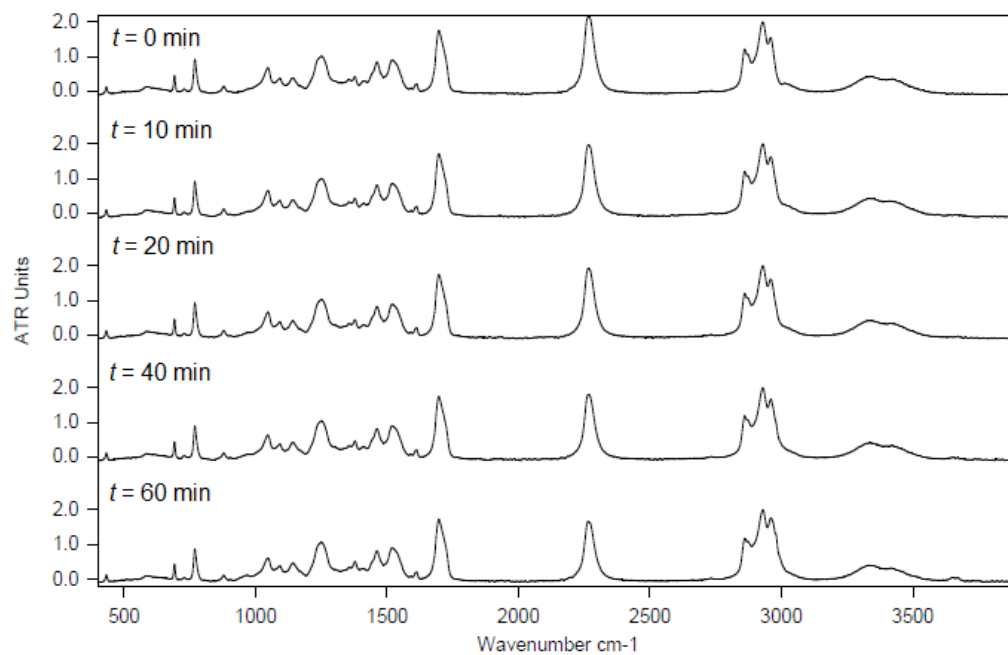
Figure S40: Catalytic reactivity of compound **1** at ambient temperature (0.05 mol% catalyst loading).
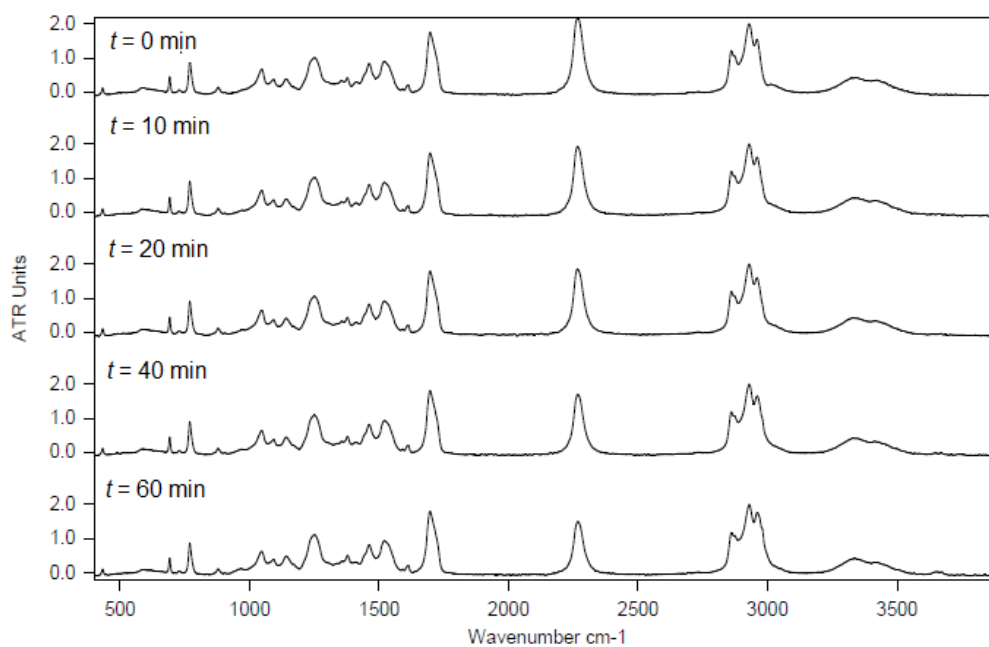
Figure S41: Catalytic reactivity of compound **2** at ambient temperature (0.05 mol% catalyst loading).
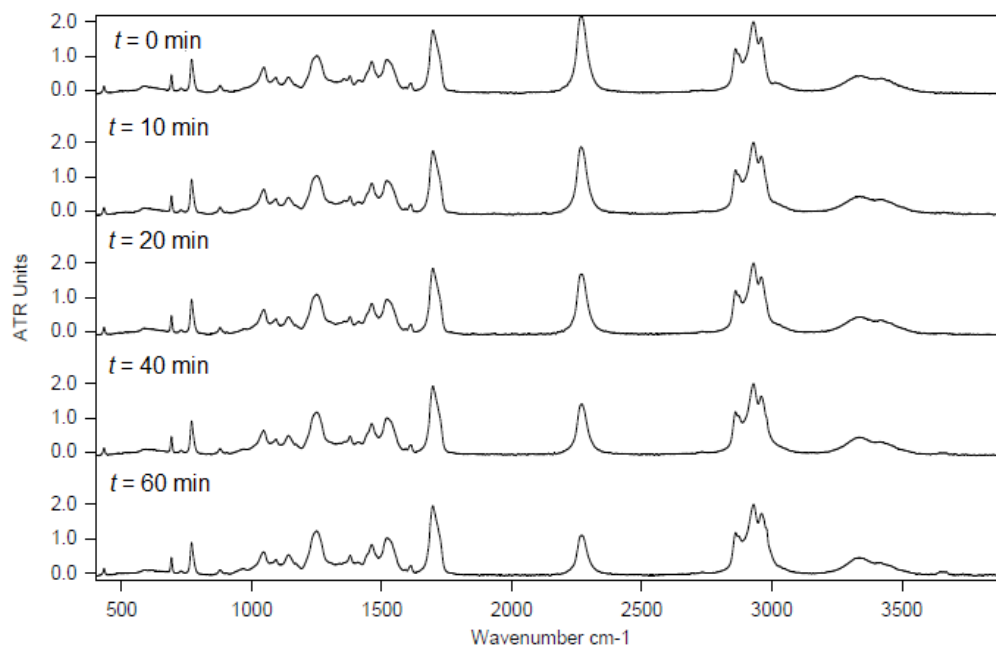
Figure S42: Catalytic reactivity of compound **3** at ambient temperature (0.05 mol% catalyst loading).
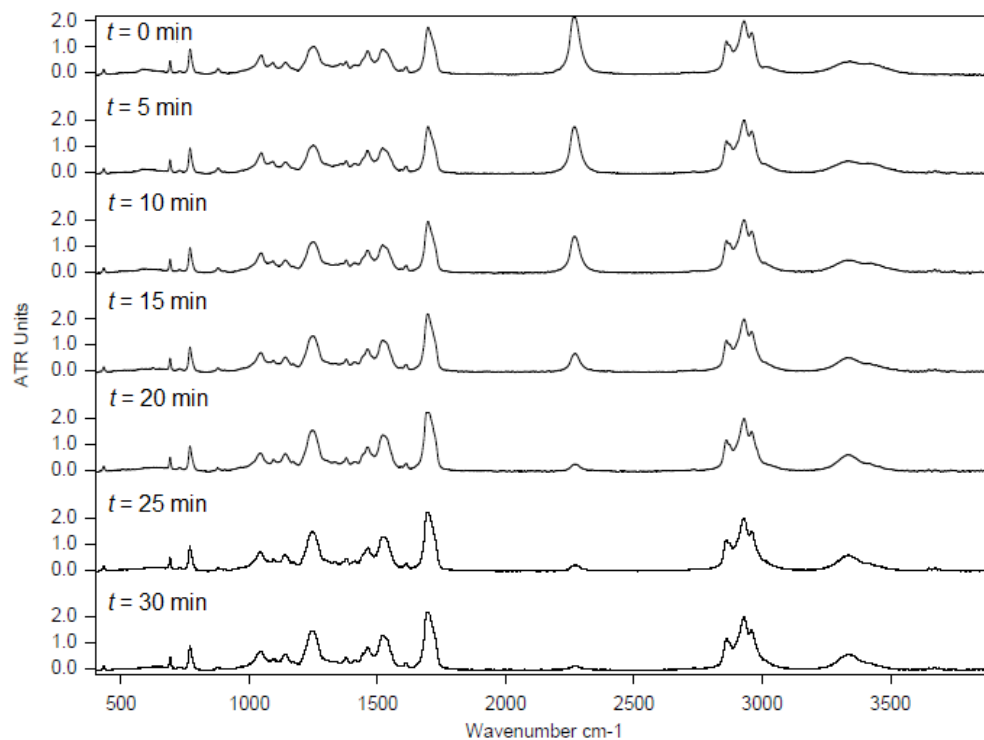
Figure S43: Catalytic reactivity of compound **7** at ambient temperature (0.05 mol% catalyst loading).
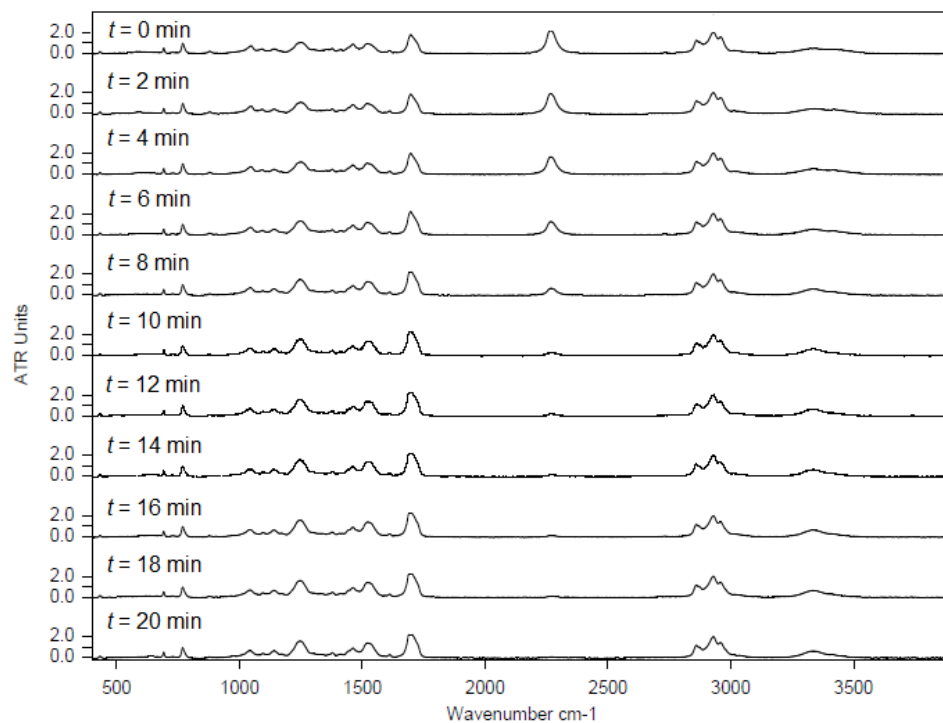
Figure S44: Catalytic reactivity of compound **8** at ambient temperature (0.05 mol% catalyst loading).
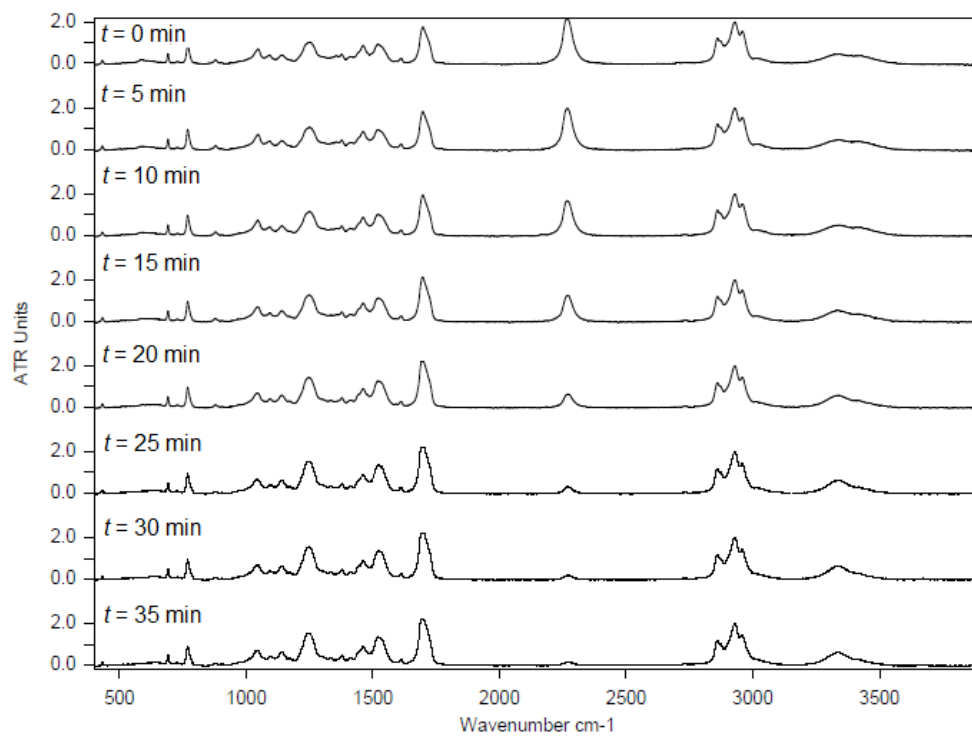
Figure S45: Catalytic reactivity of compound **9** at ambient temperature (0.05 mol% catalyst loading).
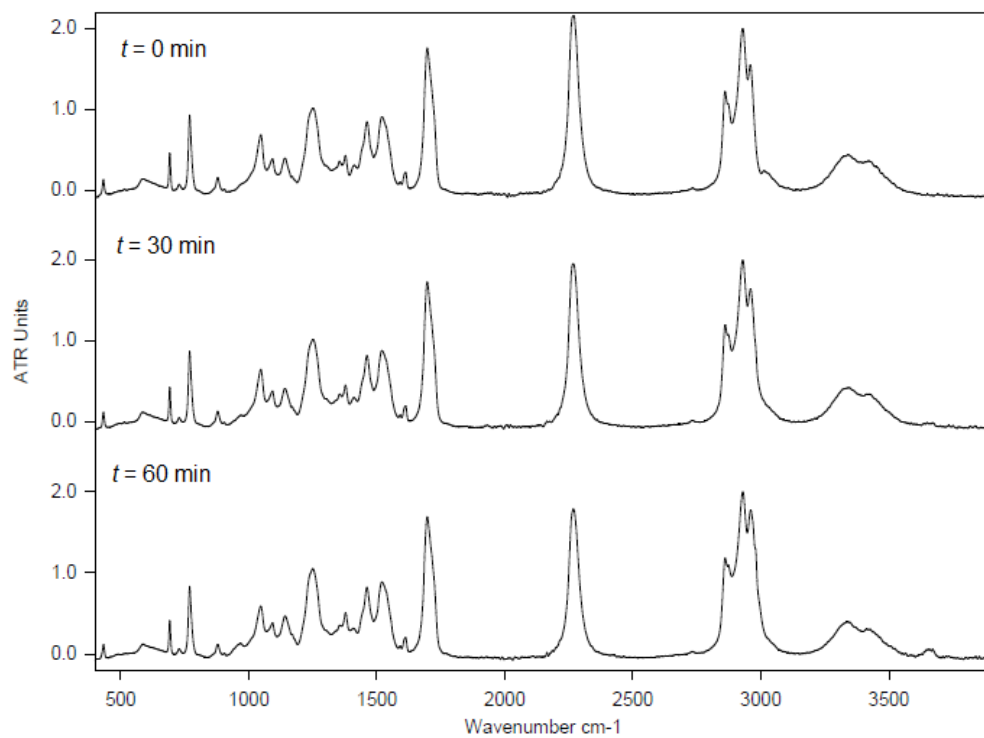
Figure S46: Catalytic reactivity of compound **4** at ambient temperature (1 mol% catalyst loading).
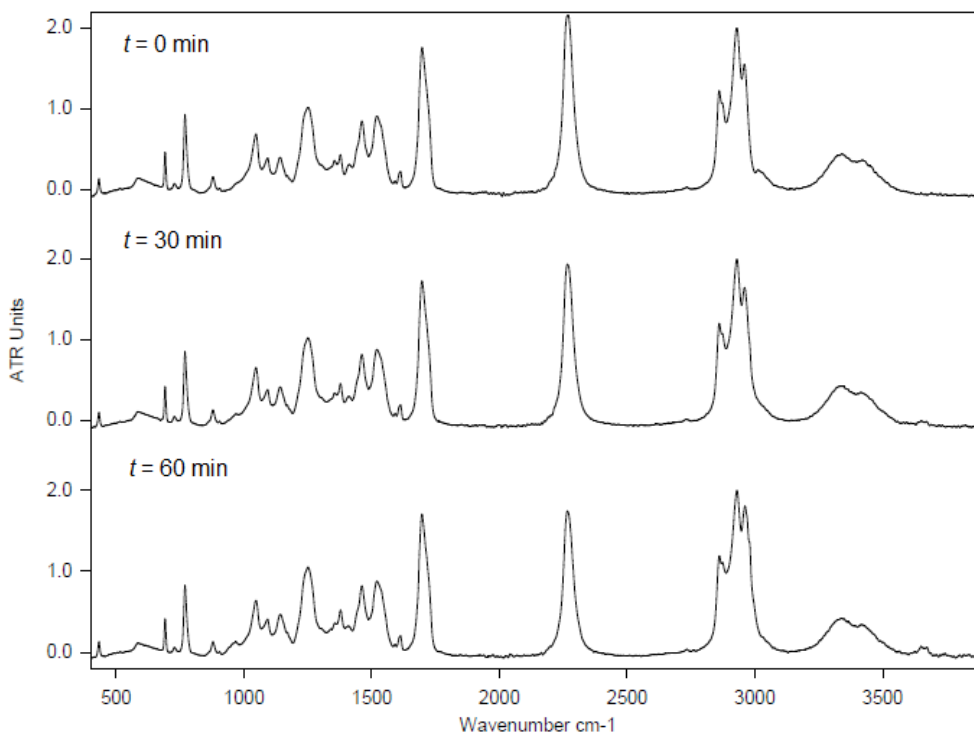
Figure S47: Catalytic reactivity of compound **5** at ambient temperature (1 mol% catalyst loading).
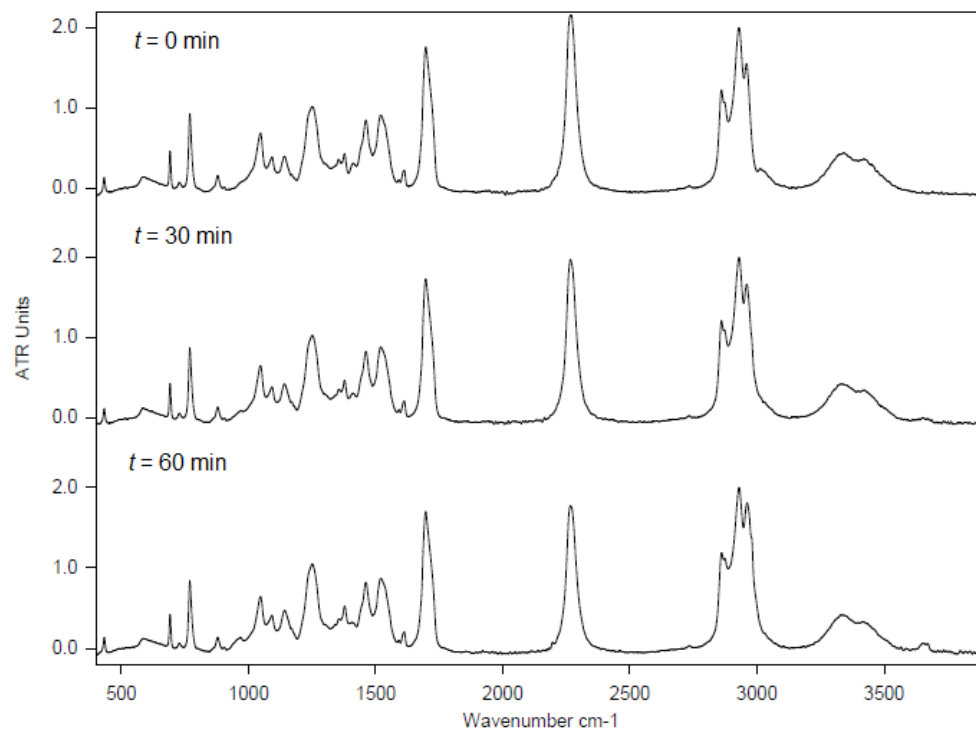
Figure S48: Catalytic reactivity of compound **6** at ambient temperature (1 mol% catalyst loading).
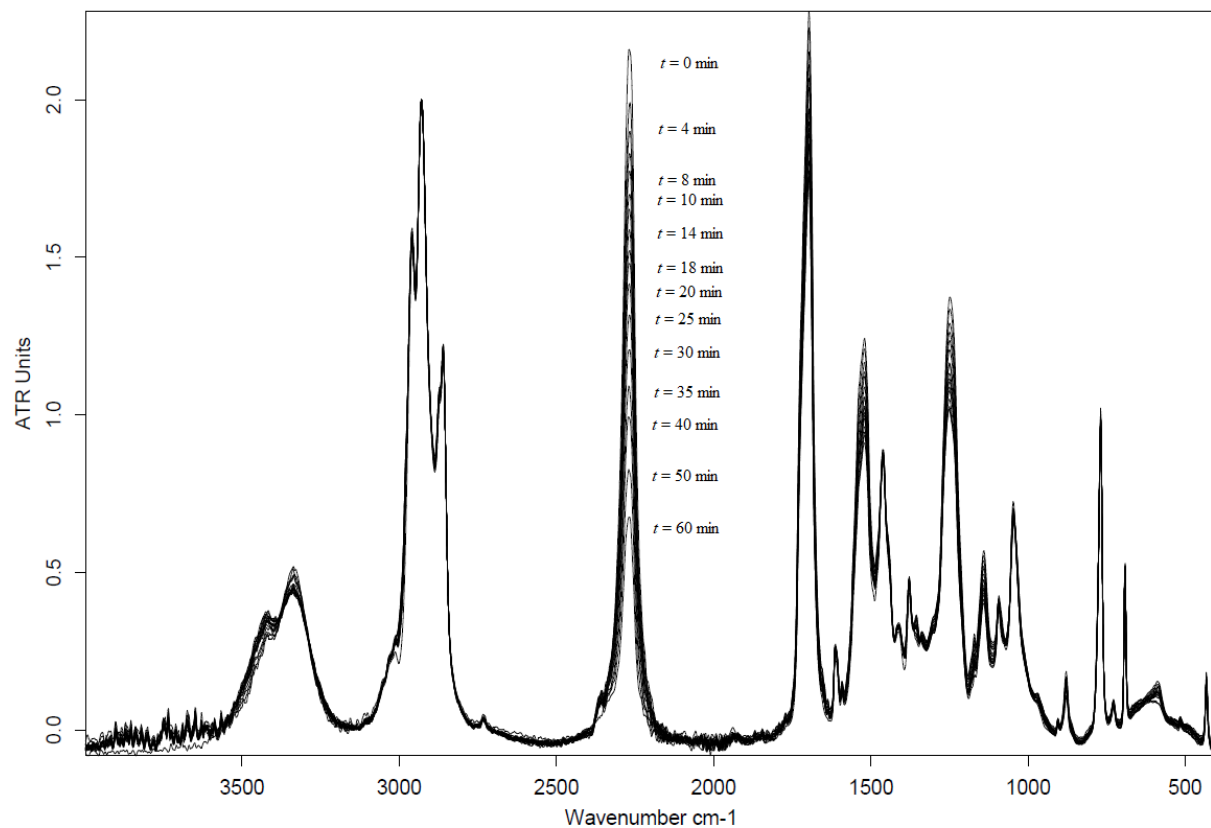
Figure S49: Catalytic reactivity of compound **3** and additionally 0.5 eq. of compound **6** at ambient temperature (0.05 mol% catalyst loading).

t = 0 min

t = 2 min

t = 4 min

t = 6 min

t = 8 min

t = 10 min

t = 14 min
t = 20 min

t = 40 min

t = 60 min
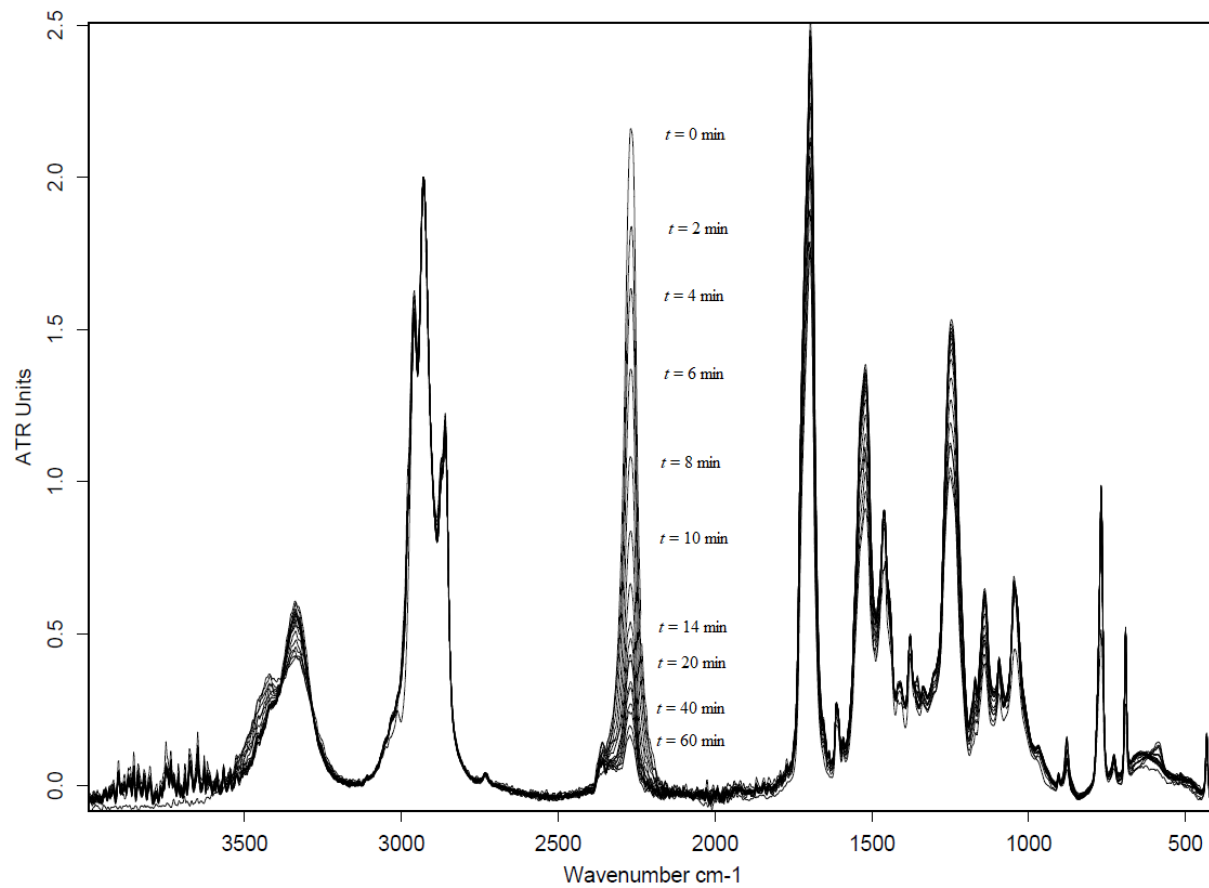
Figure S50: Catalytic reactivity of compound **3** and additionally 1.0 eq. of compound **6** at ambient temperature (0.05 mol% catalyst loading).
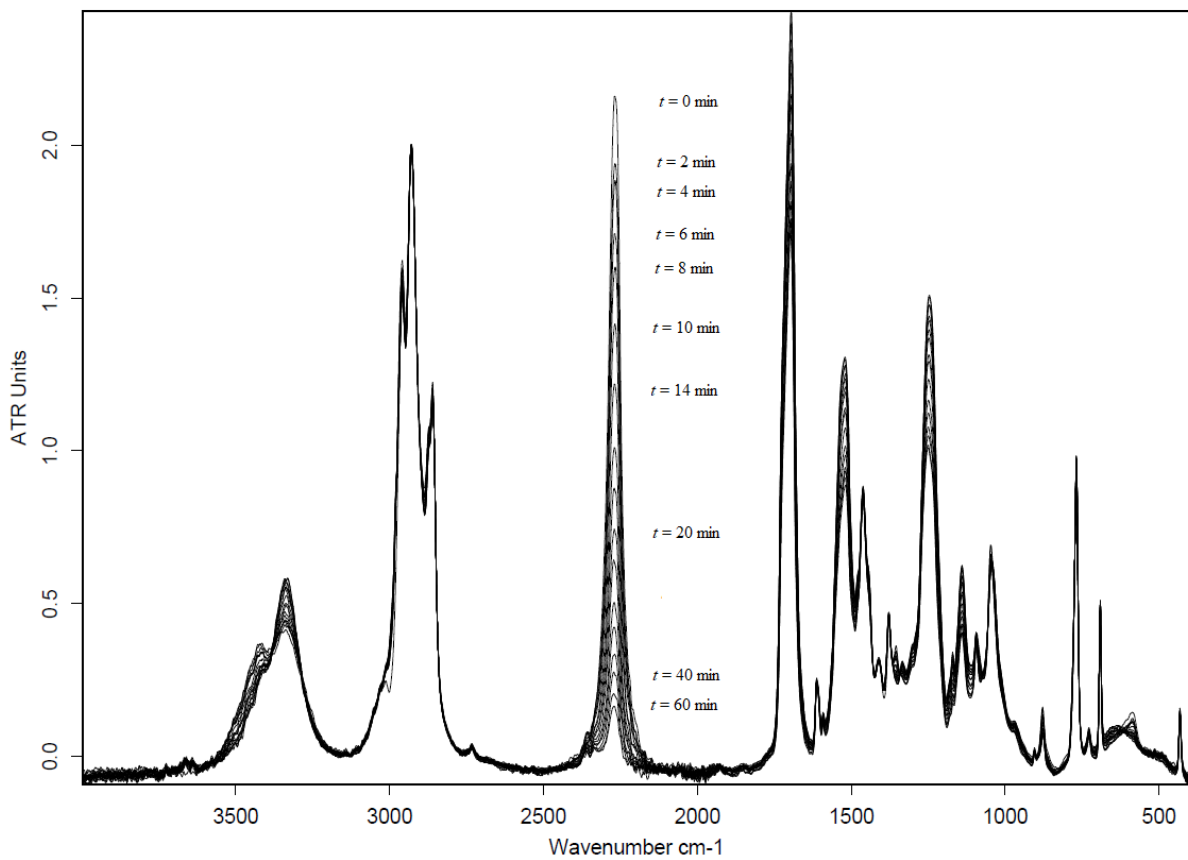
Figure S51: Catalytic reactivity of compound **3** and additionally 2.0 eq. of compound **6** at ambient temperature (0.05 mol% catalyst loading).
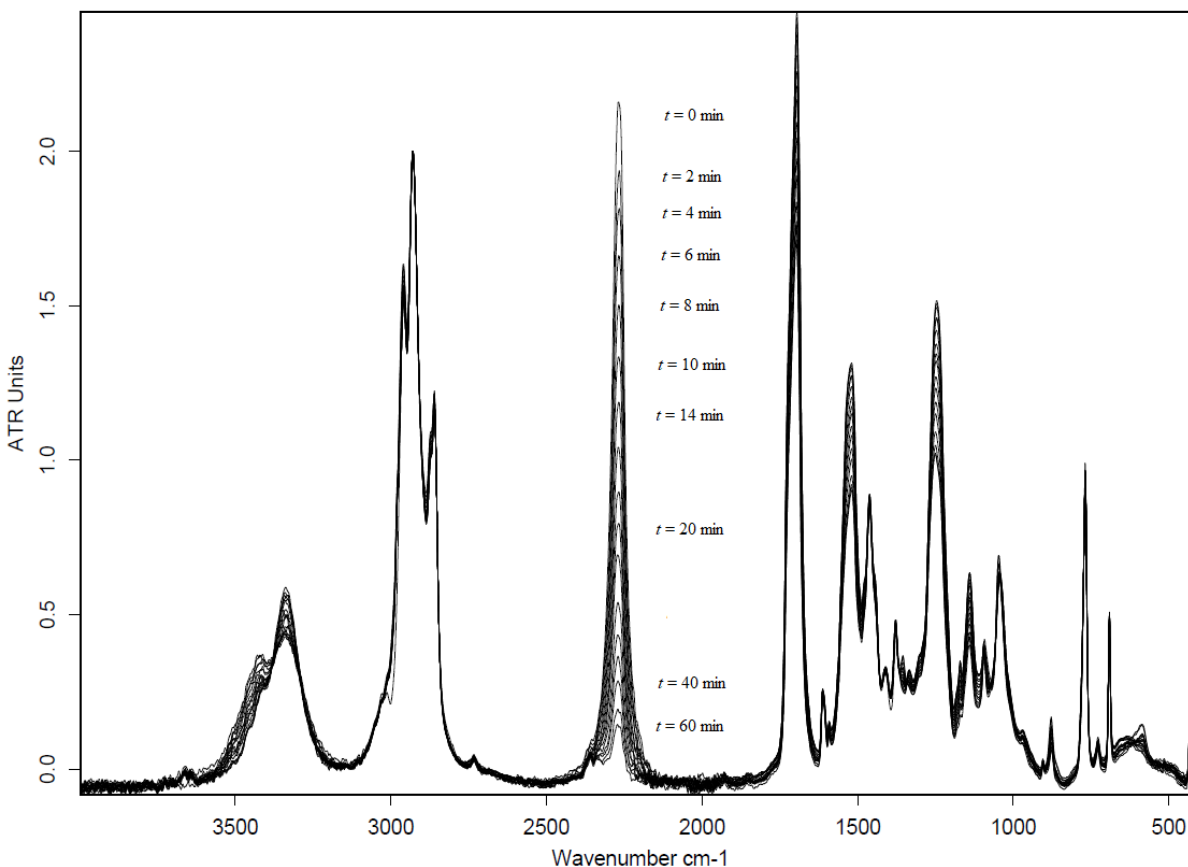
Figure S52: Catalytic reactivity of compound **3** and additionally 10.0 eq. of compound **6** at ambient temperature (0.05 mol% catalyst loading).

In order to determine the reaction order with respect to the alcohol concentration for compound **3**, the initial rate of the urethane catalysis was determined at different initial concentrations[7] and plotted logarithmically using equation **E3**

Equation E3 $\qquad log\ v_0 = log\ k + a\ log\ [\mathbf{OH}]_0$

where v_0 is the initial speed, k the rate constant, a the reaction order and $[OH]_0$ the initial concentration of the Alcohol. Reaction order results from the slope of the obtained linear gradient in case of the application of $lg(v_0)$ against $lg(c_0(OH))$. The reaction conditions and initial speeds are summarized in Table S2.

Table S2: Initial speeds of compound **1** after 60 s for urethane catalysis at ambient temperature

$c_0(NCO)$ / mol/L	$c_0(OH)$ / mol/L	v_0 / mol/(L*s)	catalyst loading / mol%
1	1	1.83×10^{-3}	0.4
1	2	2.33×10^{-3}	0.4
1	10	5.38×10^{-3}	0.4
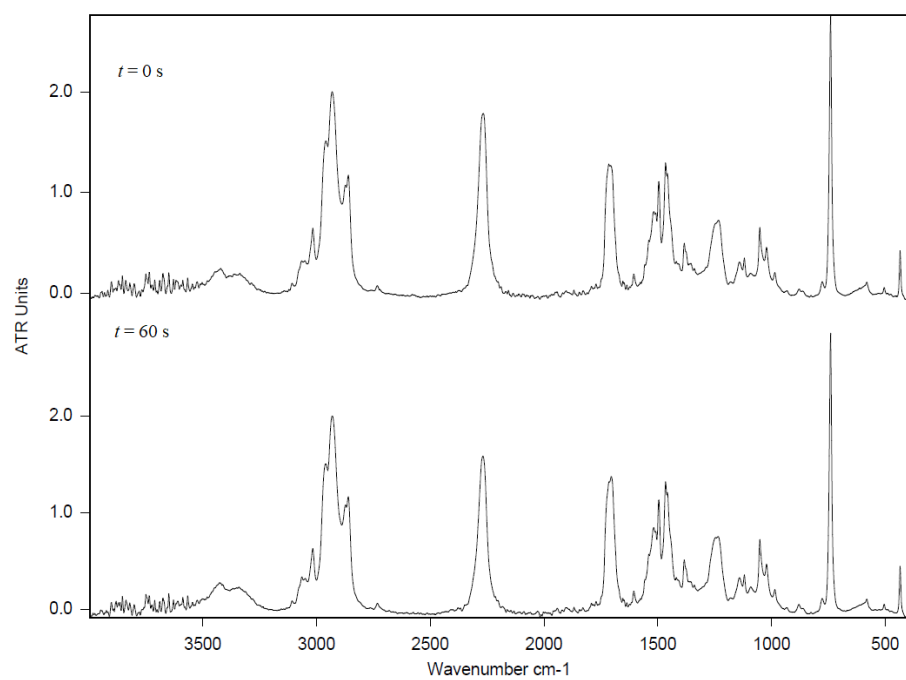
Figure S53: Catalytic reactivity of compound **1** at ambient temperature (0.4 mol% catalyst loading) and a ratio of **1 : 1 for $c_0(NCO) / c_0(OH)$**.
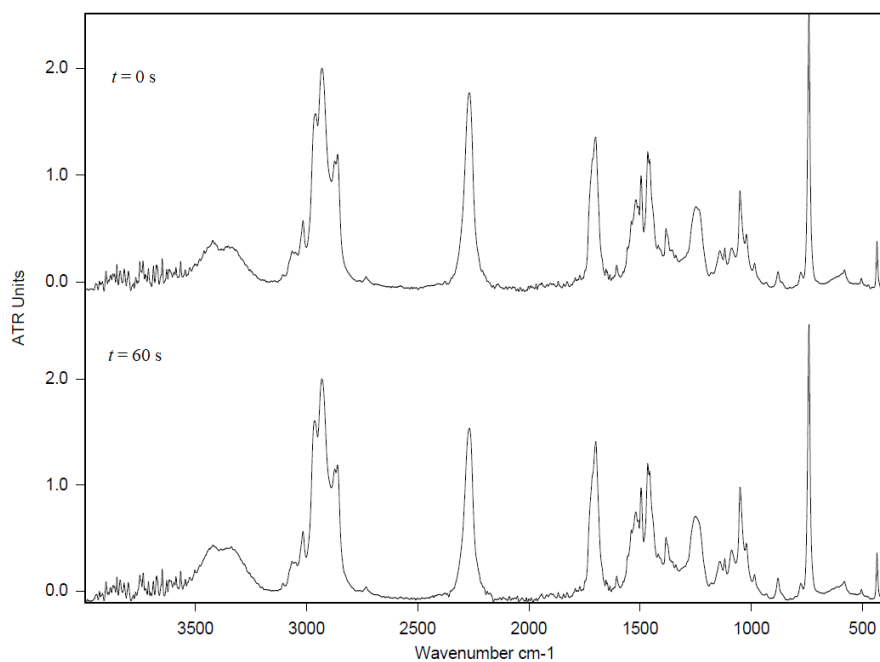
Figure S54: Catalytic reactivity of compound **1** at ambient temperature (0.4 mol% catalyst loading) and a ratio of **1 : 2 for $c_0(NCO) / c_0(OH)$**.
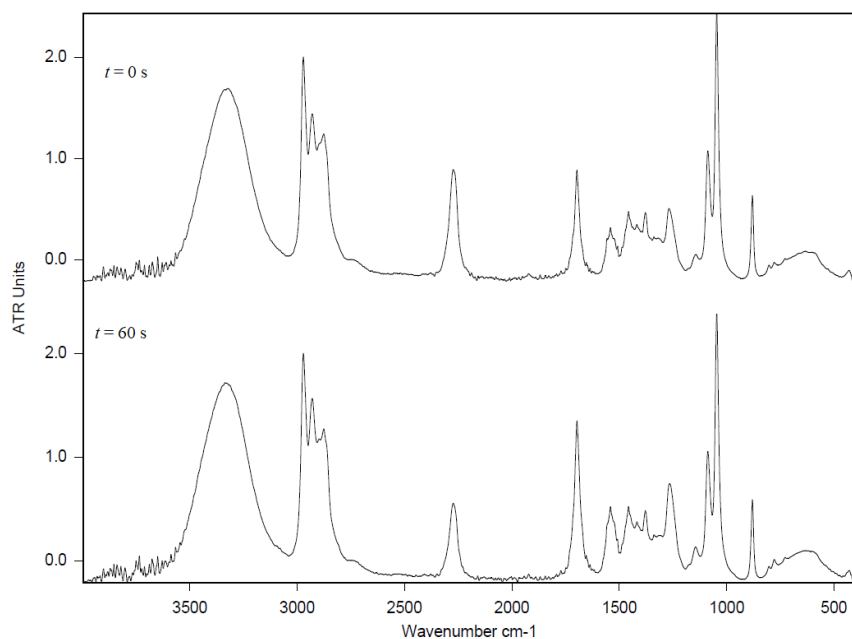
Figure S55: Catalytic reactivity of compound **1** at ambient temperature (0.4 mol% catalyst loading) and a ratio of **1 : 10 for c_0(NCO) / c_0(OH)**.
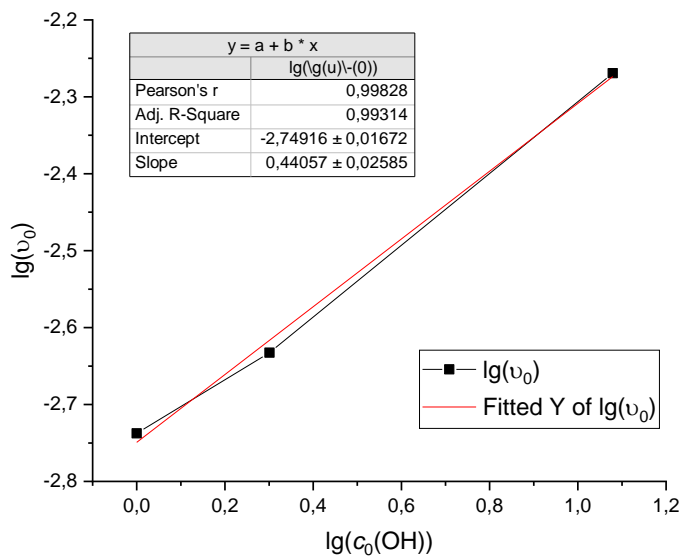
Figure S56: Determination of the reaction order regarding to EtOH of bismuth catalyzed urethane reaction. Plot of $\lg(v_0)$ against $\lg(c_0(OH))$, reaction order is obtained by the slope of the linear fit (Data from **Table S2** was used).

X-ray Diffraction Studies

General: Single-crystal X-ray diffraction data were collected on a Bruker AXS detector using Mo-K$_\alpha$ radiation (λ = 0.71073 Å). Crystals were selected under oil, mounted on glass capillaries and then immediately placed in a cold stream of N_2 on a diffractometer. Using Olex2,[8] the structures were solved with the Superflip[9–11] structure solution program using Charge Flipping or ShelXT[12] using Intrinsic Phasing and refined with the ShelXL[13] refinement package using Least Squares minimization.[14]

Ellipsoids are drawn at 50% probability. If present, solvent molecules and disordered parts are shown for a complete structural depiction.

Crystallographic data have been deposited with the Cambridge Crystallographic Data Centre as supplementary publication no. 2057615 (**3**), 2057616 (**7a**), 2057618 (**7b**), 2057617 (**8**), 2057620 (**9a**), 2057619 (**9b**).

These data can be obtained free of charge via www.ccdc.cam.uk/data_request/cif (or from the CCDC, 12 Union Road, Cambridge CB2 1EZ, UK; fax: (+44) 1223-336-033; or deposit@ccdc.cam.ac.uk).

Single-crystal X-ray structure analysis of 3:

Single crystals were obtained by storing a concentrated THF solution at -40 °C. A Single-crystal X-ray structure analysis revealed that **3** crystallizes in the triclinic space group *P*-1. The asymmetric unit contains one half of the dimer **3** with one THF molecule coordinated to Bi and one THF as solvate.
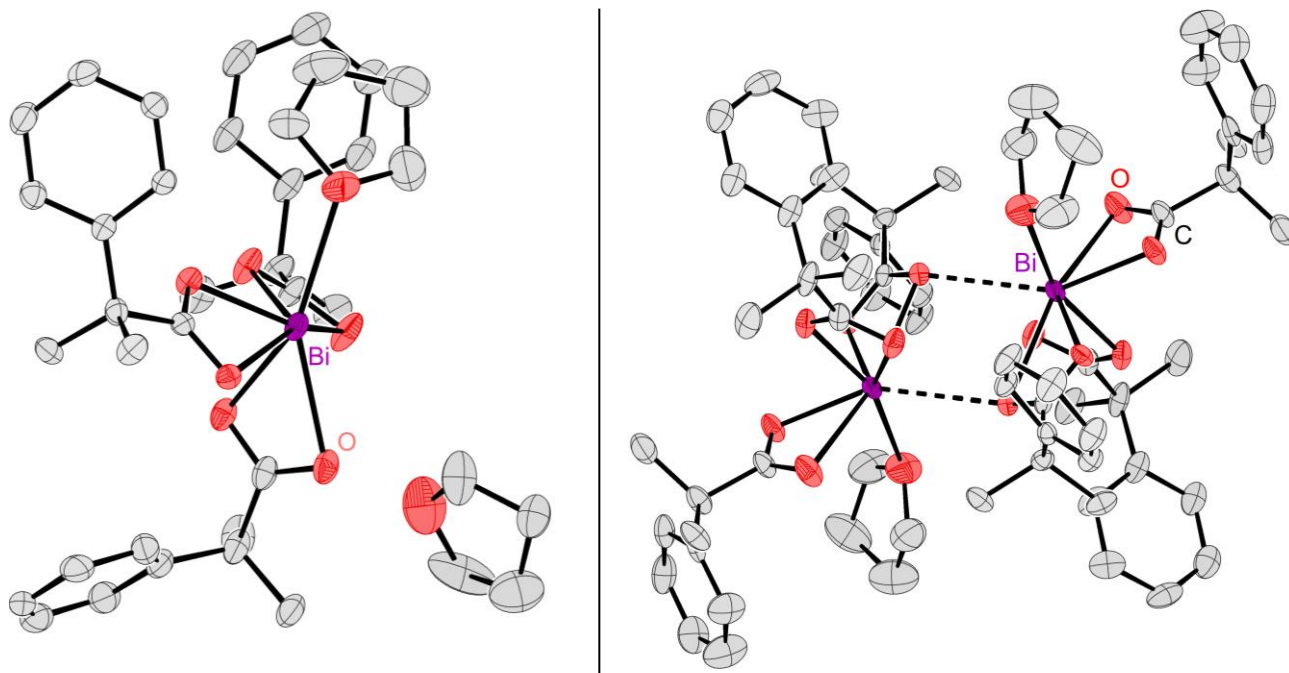
Figure S57: Molecular view of the asymmetric unit of **3** in the solid state (left). Molecular view of the dimer (right). Hydrogen atoms are omitted.

Table S3: Crystal data and structure refinement for **3**.

CCDC Number	2057615	ρ_{calc}g/cm^3	1.587
Empirical formula	C$_{38}$H$_{49}$BiO$_8$	μ/mm^{-1}	5.050
Formula weight	842.75	F(000)	848.0
Temperature/K	100(2)	Crystal size/mm^3	$0.306 \times 0.114 \times 0.089$
Crystal system	triclinic	Radiation	MoKα ($\lambda = 0.71073$)
Space group	P-1	2Θ range for data collection/°	3.508 to 56.72
a/Å	12.5878(6)	Index ranges	$-16 \leq h \leq 16, -16 \leq k \leq 16, -17 \leq l \leq 17$
b/Å	12.6544(6)	Reflections collected	27767
c/Å	13.1098(6)	Independent reflections	8719 [R$_{int}$ = 0.0550, R$_{sigma}$ = 0.0598]
α/°	106.319(3)	Data/restraints/parameters	8719/0/430
β/°	105.558(2)	Goodness-of-fit on F^2	1.079
γ/°	107.521(3)	Final R indexes [I>=2σ (I)]	R$_1$ = 0.0412, wR$_2$ = 0.0942
Volume/Å^3	1763.44(15)	Final R indexes [all data]	R$_1$ = 0.0501, wR$_2$ = 0.0985
Z	2	Largest diff. peak/hole / e Å^{-3}	2.91/-1.58

Single-crystal X-ray structure analysis of 7a-b:

Single crystals were obtained by heating a mixture of compound **1** and two equivalents of compound **4** in acetonitrile and subsequent slow cooling to room temperature. Single-crystal X-ray structure analyses revealed two polymorphs, one with acetonitrile as solvate molecule (**7b**) and one without (**7a**). Both crystallizes in the monoclinic space group $P2_1/n$. The asymmetric unit contains half a molecule of **7a/7b**.
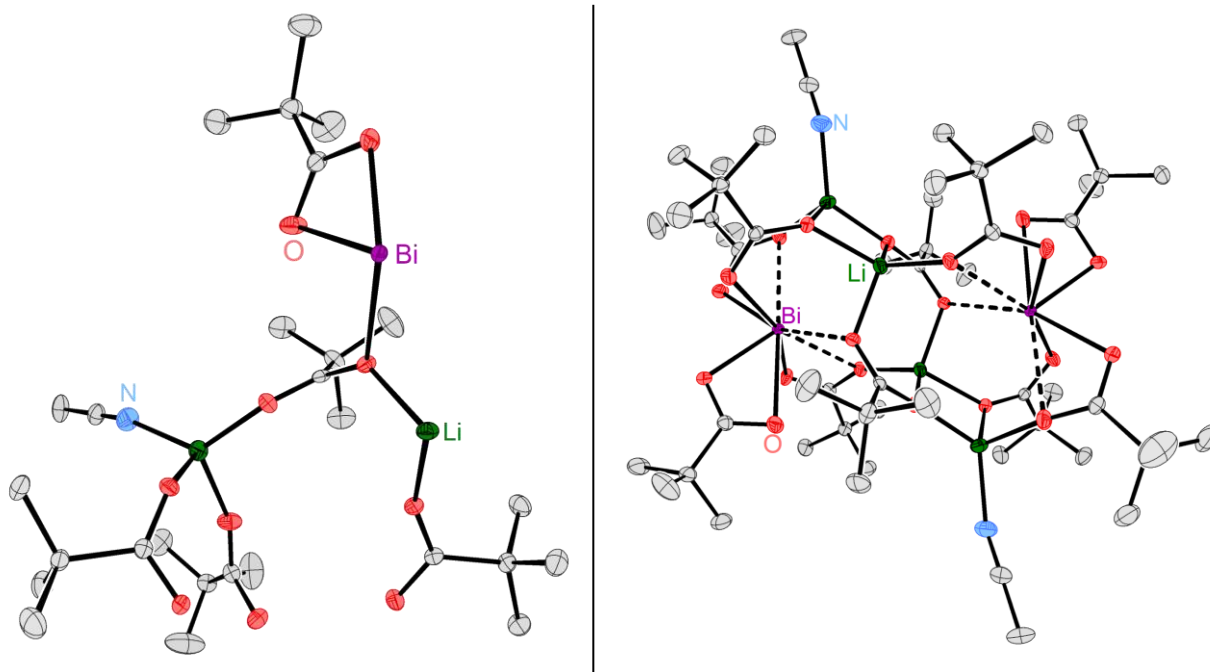
Figure S58: Molecular view of the asymmetric unit of **7a** in the solid state (left). Molecular view of the grown structure of **7a** in the solid state (right). Hydrogen atoms are omitted.

Table S4: Crystal data and structure refinement for **7a**.

CCDC Number	2057616	ρ_{calc}g/cm^3	1.467
Empirical formula	$C_{54}H_{96}Bi_2Li_4N_2O_{20}$	μ/mm^{-1}	5.109
Formula weight	1539.04	F(000)	1544.0
Temperature/K	100	Crystal size/mm^3	$0.54 \times 0.53 \times 0.28$
Crystal system	monoclinic	Radiation	MoKα ($\lambda = 0.71073$)
Space group	P2$_1$/n	2Θ range for data collection/°	3.634 to 59.212°
a/Å	13.3571(3)	Index ranges	$-18 \le h \le 18, -19 \le k \le 19, -25 \le l \le 25$
b/Å	14.0806(3)	Reflections collected	53862
c/Å	18.5930(3)	Independent reflections	9790 [R$_{int}$ = 0.0490, R$_{sigma}$ = 0.0350]
α/°	90	Data/restraints/parameters	9790/0/386
β/°	95.0534(9)	Goodness-of-fit on F^2	1.054
γ/°	90	Final R indexes [I>=2σ (I)]	R$_1$ = 0.0227, wR$_2$ = 0.0548
Volume/Å^3	3483.30(12)	Final R indexes [all data]	R$_1$ = 0.0268, wR$_2$ = 0.0562
Z	2	Largest diff. peak/hole / e Å^{-3}	1.01/-2.43
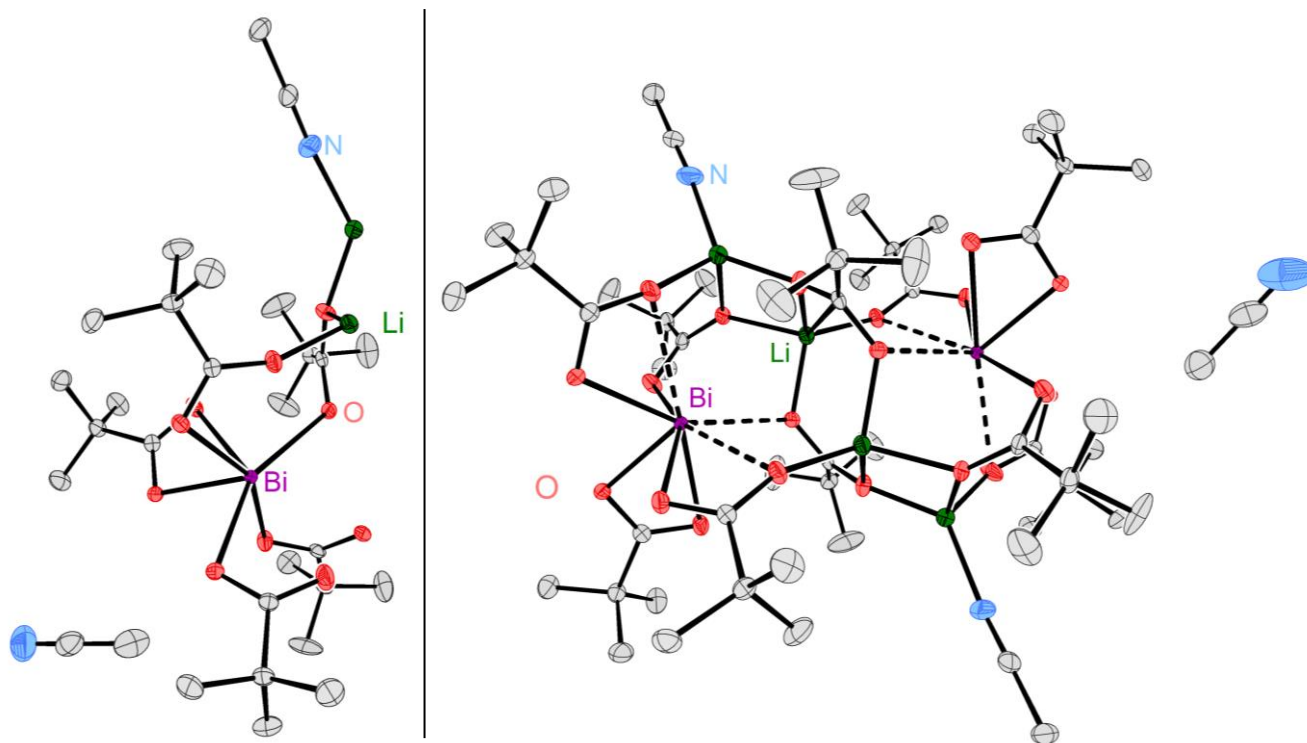
Figure S59: Molecular view of the asymmetric unit of **7b** in the solid state (left). Molecular view of the grown structure of **7b** in the solid state (right). Hydrogen atoms are omitted.

Table S5: Crystal data and structure refinement for **7b**.

CCDC Number	2057618	ρ_{calc}g/cm^3	1.441
Empirical formula	$C_{58}H_{102}Bi_2Li_4N_4O_{20}$	μ/mm^{-1}	4.769
Formula weight	1621.15	F(000)	1632.0
Temperature/K	100	Crystal size/mm^3	$0.55 \times 0.41 \times 0.29$
Crystal system	monoclinic	Radiation	MoKα (λ = 0.71073)
Space group	P2$_1$/n	2Θ range for data collection/°	2.89 to 59.134°
a/Å	16.1427(2)	Index ranges	$-22 \leq h \leq 22, -18 \leq k \leq 18, -25 \leq l \leq 25$
b/Å	13.2582(2)	Reflections collected	62925
c/Å	18.5840(2)	Independent reflections	10452 [R$_{int}$ = 0.0339, R$_{sigma}$ = 0.0234]
α/°	90	Data/restraints/parameters	10452/0/414
β/°	110.0869(6)	Goodness-of-fit on F^2	1.079
γ/°	90	Final R indexes [I>=2σ (I)]	R$_1$ = 0.0183, wR$_2$ = 0.0409
Volume/Å^3	3735.47(8)	Final R indexes [all data]	R$_1$ = 0.0215, wR$_2$ = 0.0418
Z	2	Largest diff. peak/hole / e Å^{-3}	1.31/-1.11

Single-crystal X-ray structure analysis of 8:

Single crystals were obtained by heating a mixture of compound **2** and two equivalents of compound **5** in acetonitrile and subsequent slow cooling to room temperature. A Single-crystal X-ray structure analysis revealed that **8** crystallizes in the monoclinic space group $P2_1/n$. The asymmetric unit contains half a molecule of **8**.
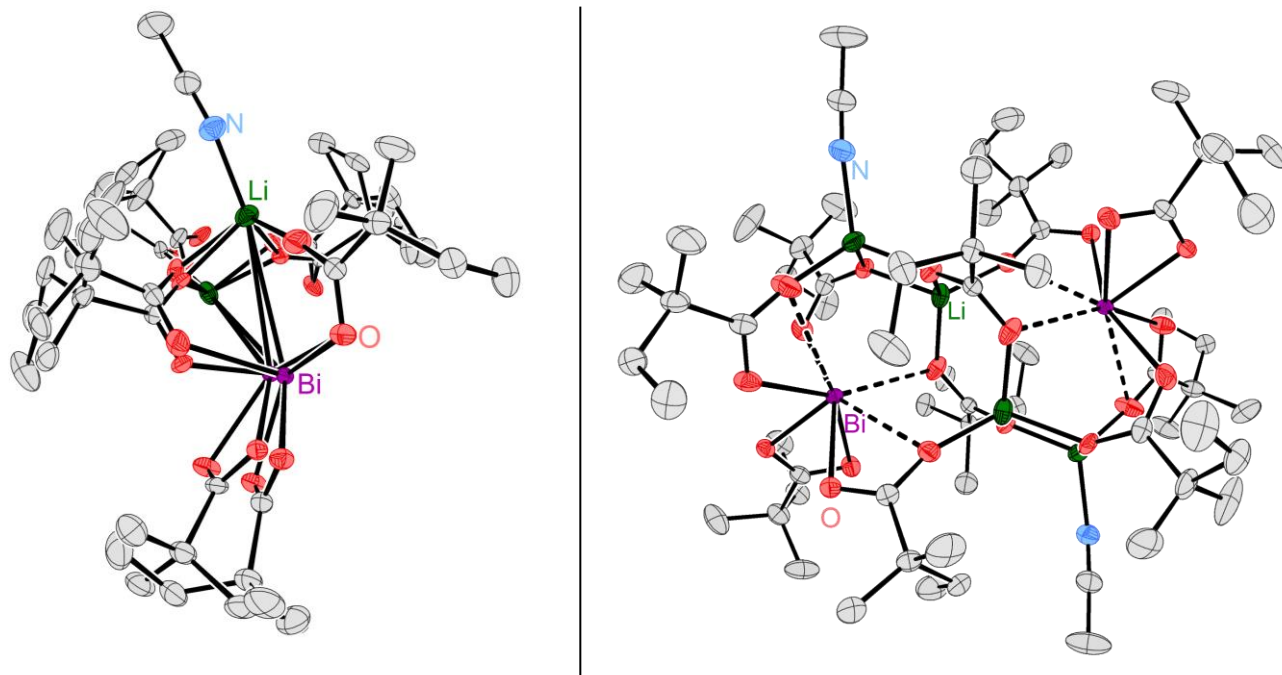
Figure S60: Molecular view of the asymmetric unit of **8** with disordered atoms (occupancy: 62% and 38%) in the solid state (left). Molecular view of the grown structure of **8** in the solid state (right; disordered atoms with lower occupancy are not depicted). Hydrogen atoms are omitted.

Table S6: Crystal data and structure refinement for **8**.

CCDC Number	2057617	ρ_{calc}g/cm^3	1.407
Empirical formula	$C_{64}H_{116}Bi_2Li_4N_2O_{20}$	μ/mm^{-1}	4.494
Formula weight	1679.30	F(000)	1704.0
Temperature/K	100	Crystal size/mm^3	$0.39 \times 0.28 \times 0.19$
Crystal system	monoclinic	Radiation	MoKα ($\lambda = 0.71073$)
Space group	P2$_1$/n	2Θ range for data collection/°	3.49 to 60.202°
a/Å	14.3713(2)	Index ranges	$-20 \leq h \leq 20, -25 \leq k \leq 25, -21 \leq l \leq 21$
b/Å	17.9791(2)	Reflections collected	68981
c/Å	15.3608(2)	Independent reflections	11639 [$R_{int} = 0.0288$, $R_{sigma} = 0.0195$]
α/°	90	Data/restraints/parameters	11639/18/701
β/°	92.5080(10)	Goodness-of-fit on F^2	1.012
γ/°	90	Final R indexes [I>=2σ (I)]	R$_1$ = 0.0182, wR$_2$ = 0.0413
Volume/Å^3	3965.17(9)	Final R indexes [all data]	R$_1$ = 0.0224, wR$_2$ = 0.0429
Z	2	Largest diff. peak/hole / e Å^{-3}	1.00/-1.03

Single-crystal X-ray structure analysis of 9a-b:

Single crystals were obtained by heating a mixture of compound **3** and two equivalents of compound **6** in acetonitrile and subsequent slow cooling to room temperature. Single-crystal X-ray structure analyses revealed two polymorphs, one with acetonitrile as solvate molecule (**9b**) and one without (**9a**). Both crystallizes in the monoclinic space group $P2_1/c$. The asymmetric unit contains two half molecules of **9a** / **9b**.
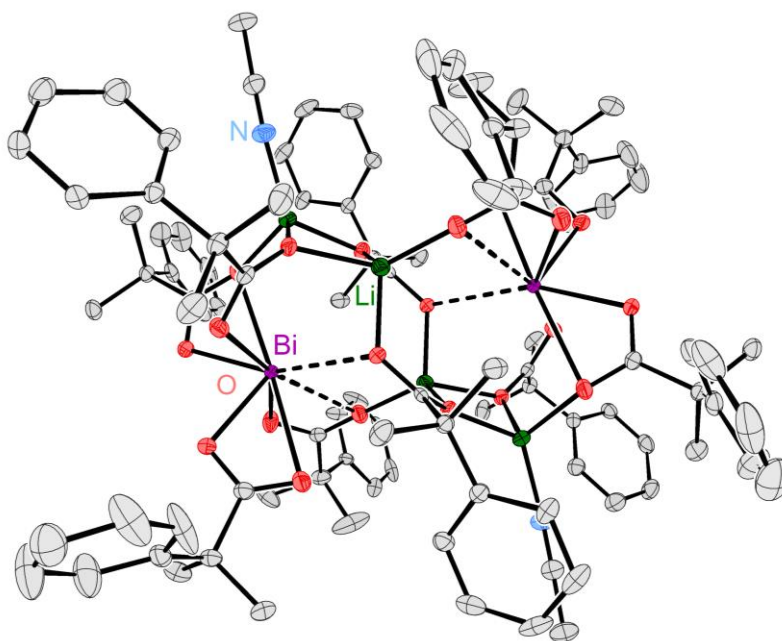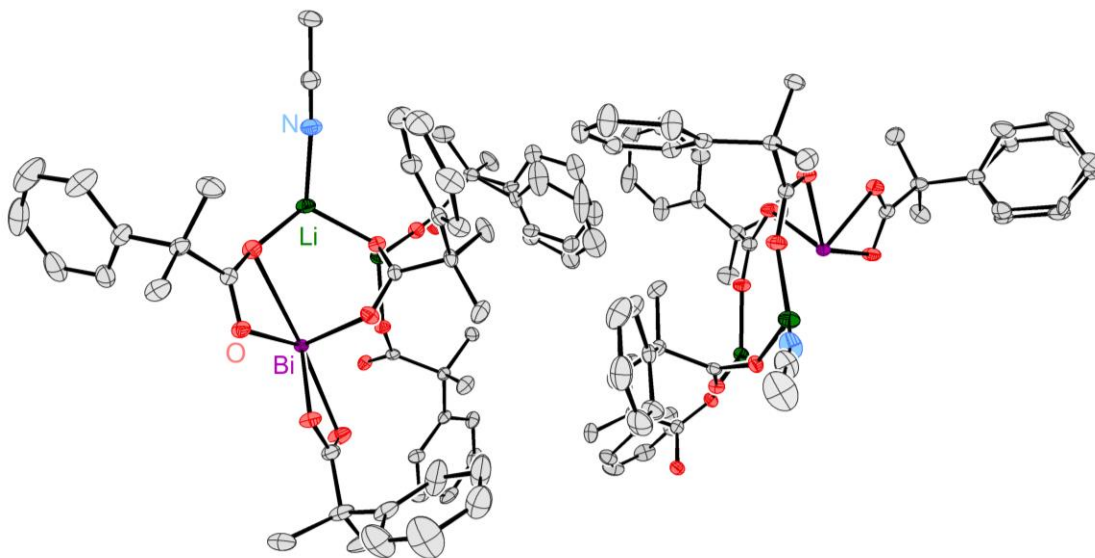
Figure S61: Molecular view of the asymmetric unit of **9a** with disordered atoms (occupancy 68% and 32%) in the solid state (top). Molecular view of one Bi_2Li_4 cluster (bottom; disordered atoms with lower occupancy are omitted). Hydrogen atoms are omitted.

Table S7: Crystal data and structure refinement for **9a**.

CCDC Number	2057620	$\rho_{calc}g/cm^3$	1.463
Empirical formula	$C_{104}H_{116}Bi_2Li_4N_2O_{20}$	μ/mm^{-1}	3.654
Formula weight	2159.70	F(000)	4368.0
Temperature/K	100	Crystal size/mm^3	$0.24 \times 0.16 \times 0.16$
Crystal system	monoclinic	Radiation	MoKα ($\lambda = 0.71073$)
Space group	P2$_1$/c	2Θ range for data collection/°	2.994 to 59.172
a/Å	24.7978(8)	Index ranges	$-34 \leq h \leq 34, -22 \leq k \leq 22, -34 \leq l \leq 34$
b/Å	16.4792(5)	Reflections collected	166661
c/Å	24.6871(8)	Independent reflections	27497 [R$_{int}$ = 0.0346, R$_{sigma}$ = 0.0235]
α/°	90	Data/restraints/parameters	27497/24/1312
β/°	103.6240(10)	Goodness-of-fit on F^2	1.015
γ/°	90	Final R indexes [I>=2σ (I)]	R$_1$ = 0.0235, wR$_2$ = 0.0501
Volume/Å^3	9804.5(5)	Final R indexes [all data]	R$_1$ = 0.0335, wR$_2$ = 0.0530
Z	4	Largest diff. peak/hole / e Å^{-3}	1.26/-0.50
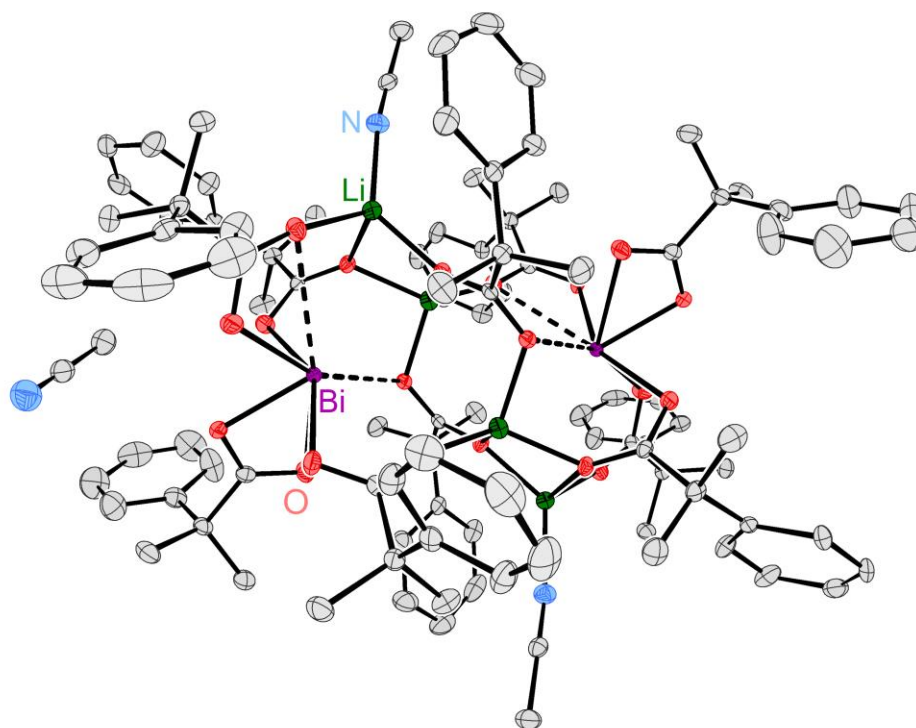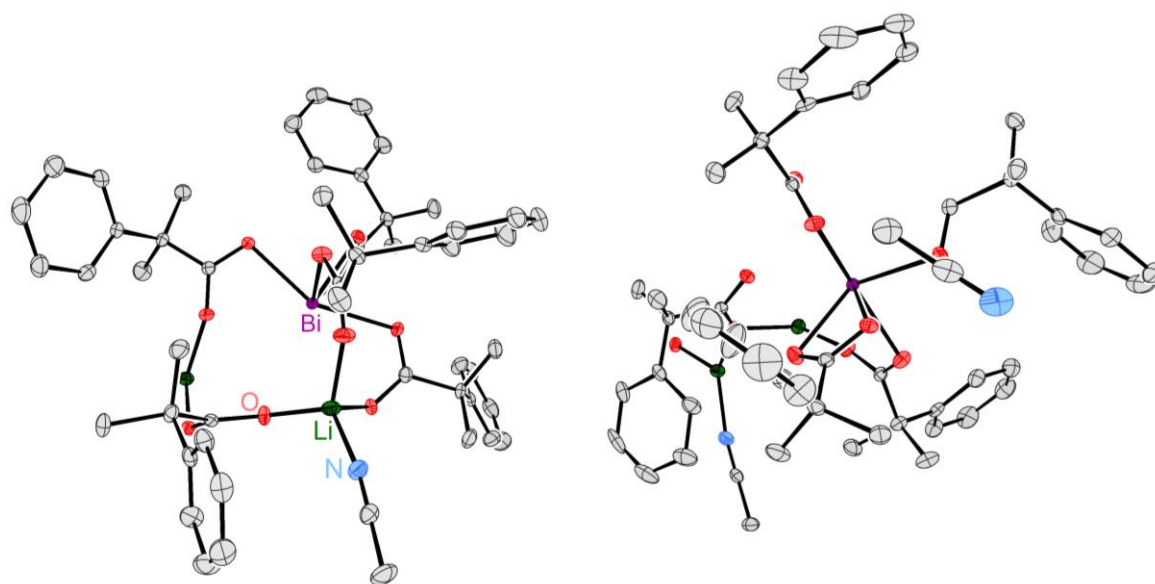
Figure S62: Molecular view of the asymmetric unit of **9b** in the solid state (top). Molecular view of one Bi_2Li_4 cluster in the solid state (bottom). Hydrogen atoms are omitted.

Table S8: Crystal data and structure refinement for **9b**.

CCDC Number	2057619	ρ_{calc}g/cm^3	1.443
Empirical formula	$C_{106}H_{119}Bi_2Li_4N_3O_{20}$	μ/mm^{-1}	3.539
Formula weight	2200.75	F(000)	4456.0
Temperature/K	100	Crystal size/mm^3	$0.6 \times 0.581 \times 0.574$
Crystal system	monoclinic	Radiation	MoKα ($\lambda = 0.71073$)
Space group	P2$_1$/c	2Θ range for data collection/°	2.746 to 59.226
a/Å	24.0601(12)	Index ranges	$-33 \leq h \leq 33, -26 \leq k \leq 26, -31 \leq l \leq 30$
b/Å	18.8535(9)	Reflections collected	171165
c/Å	22.3563(12)	Independent reflections	28447 [$R_{int} = 0.0756$, $R_{sigma} = 0.0539$]
α/°	90	Data/restraints/parameters	28447/0/1238
β/°	92.989(3)	Goodness-of-fit on F^2	1.031
γ/°	90	Final R indexes [I>=2σ (I)]	$R_1 = 0.0298$, $wR_2 = 0.0669$
Volume/Å^3	10127.4(9)	Final R indexes [all data]	$R_1 = 0.0385$, $wR_2 = 0.0700$
Z	4	Largest diff. peak/hole / e Å^{-3}	1.90/-1.63

DFT Calculations

All equilibrium and transition state structures were optimized using the BP86[15,16] and M06-2X[17] density functional methods employing Ahlrichs basis sets (def(2)-TZVP(P))[18]. All calculations were performed with the Turbomole package of programs (version 7.2)[19]. The transition state were searched by following the negative eigenvalue vector of guess structures, followed by an internal reaction coordinate analysis. The solvent effect was represented utilizing the conductor-like screening model (COSMO) with default parameter settings and ε=infinity[20]. Thermodynamic contributions to the electronic energies, taking into account solvent effects, are calculated using COSMO-RS[21](version 17) at 25°C. We report free energies ΔG obtained for 298.15 K and 1 atmosphere with harmonic frequencies. The model solvent consists of 4-((propylcarbamoyl)oxy)butyl propionate, representing specific reaction mixtures under consideration.

References

1   A. P. M. Robertson, N. Burford, R. McDonald and M. J. Ferguson, *Angewandte Chemie (International ed. in English)*, 2014, **53**, 3480–3483.

2   P. C. Andrews, G. B. Deacon, P. C. Junk, I. Kumar and M. Silberstein, *Dalton Trans.*, 2006, 4852–4858.

3   M. D. Pelta, G. A. Morris, M. J. Stchedroff and S. J. Hammond, *Magnetic Resonance in Chemistry*, 2002, **40**, S147-S152.

4   A. Macchioni, G. Ciancaleoni, C. Zuccaccia and D. Zuccaccia, *Chem. Soc. Rev.*, 2008, **37**, 479–489.

5   D. Ben-Amotz and K. G. Willis, *J. Phys. Chem.*, 1993, **97**, 7736–7742.

6   T. Hatanpää, M. Vehkamäki, M. Ritala and M. Leskelä, *Dalton Trans.*, 2010, **39**, 3219–3226.

7   P. W. Atkins and J. de Paula, *Atkins' physical chemistry*, Oxford Univ. Press, Oxford, 8th edn., 2006.

8   O. V. Dolomanov, L. J. Bourhis, R. J. Gildea, J. A. K. Howard and H. Puschmann, *J. Appl. Cryst.*, 2009, **42**, 339–341.

9   L. Palatinus and A. van der Lee, *J. Appl. Cryst.*, 2008, **41**, 975–984.

10 L. Palatinus and G. Chapuis, *J. Appl. Cryst.*, 2007, **40**, 786–790.

11 L. Palatinus, S. J. Prathapa and S. van Smaalen, *J. Appl. Cryst.*, 2012, **45**, 575–580.

12 G. M. Sheldrick, *Acta Cryst. A*, 2015, **71**, 3–8.

13 G. M. Sheldrick, *Acta Cryst. C*, 2015, **71**, 3–8.

14 G. M. Sheldrick, *Acta Cryst. A*, 2008, **64**, 112–122.

15 Perdew, *Phys. Rev. B*, 1986, **33**, 8822–8824.

16 Perdew and Yue, *Phys. Rev. B*, 1986, **33**, 8800–8802.

17 Y. Zhao and D. G. Truhlar, *J. Chem. Theory. Comput.*, 2008, **4**, 1849–1868.

18 A. Schäfer, C. Huber and R. Ahlrichs, *J. Chem. Phys.*, 1994, **100**, 5829–5835.

19 R. Ahlrichs, M. Bär, M. Häser, H. Horn and C. Kölmel, *Chem. Phys. Lett.*, 1989, **162**, 165–169.

20 A. Klamt and G. Schüürmann, *J. Chem. Soc., Perkin Trans. 2*, 1993, **0**, 799–805.

21 A. Klamt, *J. Phys. Chem.*, 1995, **99**, 2224–2235.